AD-A156 907 POSSIBLE CROSS EQUATORIAL INFLUENCE OF THE NORTHEAST MONSOON ON THE EQUATORIAL WESTERLIES OVER INDONESIA(U) NAVAL POSTGRADUATE SCHOOL MONTEREY CA K A SHIELD 1/1

UNCLASSIFIED MAR 85 F/G 4/2 NL

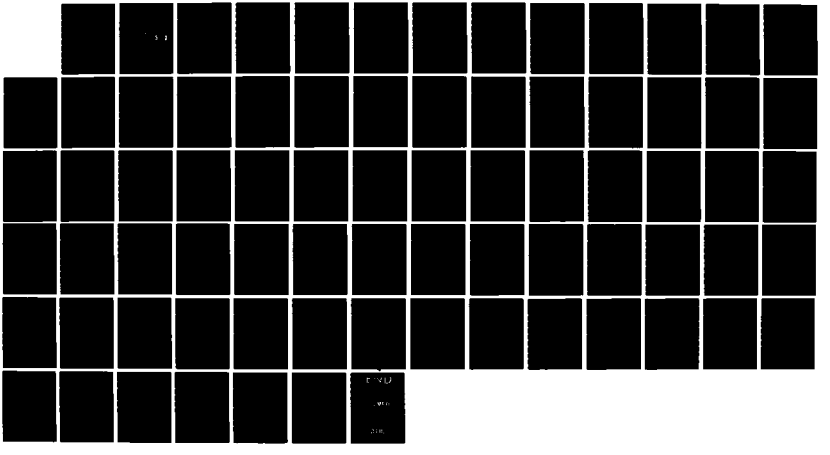

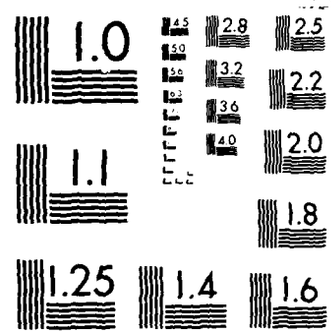

(2)

NAVAL POSTGRADUATE SCHOOL

Monterey, California

THESIS

POSSIBLE CROSS EQUATORIAL INFLUENCE
OF THE NORTHEAST MONSOON
ON THE EQUATORIAL WESTERLIES OVER INDONESIA

by

Kathy A. Shield

March 1985

Thesis Advisor: C.-P. Chang

Approved for public release; distribution unlimited.

UNCLASSIFIED

SECURITY CLASSIFICATION OF THIS PAGE (When Data Entered)

REPORT DOCUMENTATION PAGE		READ INSTRUCTIONS BEFORE COMPLETING FORM
1. REPORT NUMBER	2. GOVT ACCESSION NO.	3. RECIPIENT'S CATALOG NUMBER
4. TITLE (and Subtitle) Possible Cross Equatorial Influence of the Northeast Monsoon on the Equatorial Westerlies over Indonesia		5. TYPE OF REPORT & PERIOD COVERED Master's Thesis March 1985 6. PERFORMING ORG. REPORT NUMBER
7. AUTHOR(s) Kathy A. Shield		8. CONTRACT OR GRANT NUMBER(s)
9. PERFORMING ORGANIZATION NAME AND ADDRESS Naval Postgraduate School Monterey, California 93943		10. PROGRAM ELEMENT, PROJECT, TASK AREA & WORK UNIT NUMBERS
11. CONTROLLING OFFICE NAME AND ADDRESS Naval Postgraduate School Monterey, California 93943		12. REPORT DATE March 1985 13. NUMBER OF PAGES 73
14. MONITORING AGENCY NAME & ADDRESS(if different from Controlling Office)		15. SECURITY CLASS. (of this report) Unclassified 15a. DECLASSIFICATION/DOWNGRADING SCHEDULE

16. DISTRIBUTION STATEMENT (of this Report)

Approved for public release; distribution unlimited

17. DISTRIBUTION STATEMENT (of the abstract entered in Block 20, if different from Report)

18. SUPPLEMENTARY NOTES

19. KEY WORDS (Continue on reverse side if necessary and identify by block number)

Cross Equatorial Flow
Southern Summer Monsoon
Interhemispheric Influence
Monsoon Onset
Australian Monsoon
Tropical-Midlatitude Influence

20. ABSTRACT (Continue on reverse side if necessary and identify by block number)

Objectively analysed surface, 700 and 200 mb winds of nine winters are used to study the possible cross equatorial influence of the northern winter monsoon on the zonal wind along 10°S in the Indonesia-Arafura Sea region and to prepare a nine-year monthly mean climatology. Key circulation features are represented by area averaged and time composited parameters in an attempt to infer correlations between their

DD FORM 1 JAN 73 1473 EDITION OF 1 NOV 65 IS OBSOLETE

S/N 0102-LF-014-6601

UNCLASSIFIED

SECURITY CLASSIFICATION OF THIS PAGE (When Data Entered)

#20 - ABSTRACT - (CONTINUED)

perturbations. Specifically, the acceleration of the zonal wind along 10°S in the Indonesia-Arafura Sea region is used to define the onset of the southern summer monsoon and illustrate the timing between circulation features of interest in both hemispheres. While no conclusive results were achieved, some basic observations can be made. Mid-season active phases in the southern summer monsoon appear to be influenced by surges in the northeast monsoon in the Northern Hemisphere while late season events appear to be primarily a result of Southern Hemispheric, mid-latitude, baroclinic effects. In both cases, the meridional extent of the southern summer monsoon is limited. Even in the mid-season event, variability in area-averaged cross equatorial flow may not be indicative of the nature of forcing of the Northern Hemisphere's monsoonal winds on the southern summer monsoonal winds along 10°S.

Approved for public release; distribution is unlimited.

Possible Cross Equatorial Influence of the Northeast Monsoon on the Equatorial Westerlies over Indonesia

by

Kathy A. Shield
Lieutenant, United States Navy
B.A., Cakland University, 1977

Submitted in partial fulfillment of the
requirements for the degree of

MASTER OF SCIENCE IN METEORLOLOGY AND OCEANOGRAPHY

from the

NAVAL POSTGRADUATE SCHOOL
March 1985

Author: _____
Kathy A. Shield

Approved by: _____
C.-P. Chang, Thesis Advisor

_____
J.S. Boyle, Co-Advisor

_____
Robert J. Renard, Chairman,
Department of Meteorology

_____
John N. Dyer,
Dean of Science and Engineering

ABSTRACT

Objectively analysed surface, 700 and 200 mb winds of nine winters are used to study the possible cross equatorial influence of the northern winter monsoon on the zonal wind along 10°S in the Indonesia-Arafura Sea region and to prepare a nine year monthly mean climatology. Key circulation features are represented by area averaged and time composited parameters in an attempt to infer correlations between their perturbations. Specifically, the acceleration of the zonal wind along 10°S in the Indonesia-Arafura Sea region is used to define the onset of the southern summer monsoon and illustrate the timing between circulation features of interest in both hemispheres. While no conclusive results were achieved, some basic observations can be made. Mid-season active phases in the southern summer monsoon appear to be influenced by surges in the northeast monsoon in the Northern Hemisphere while late season events appear to be primarily a result of Southern Hemispheric, mid-latitude, baroclinic effects. In both cases, the meridional extent of the southern summer monsoon is limited. Even in the mid-season event, variability in area-averaged cross equatorial flow may not be indicative of the nature of forcing of the Northern Hemisphere's monsoonal winds on the southern summer monsoonal winds along 10°S.

TABLE OF CONTENTS

LIST OF TABLES

LIST OF FIGURES

ACKNOWLEDGEMENTS

Special thanks to Drs. C.-P. Chang and J.S. Boyle for their invaluable guidance in the preparation of this thesis. I wish to thank Drs. M.S. Peng and M.A. Rennick who provided assistance and suggestions in various phases of this study. This research was supported in part by the National Science Foundation under Grant ATM-8315175.

I. INTRODUCTION

The monsoons in the North Hemisphere, whether the northeast (northern winter) or the southwest (northern summer), have been extensively studied by a large number of metecrologists, while the monsoons of the South Hemisphere have received much less attention except by scientists in the region directly influenced by them. Early documentation of the nature of the summer monsocnal circulation over northern Australia was primarily done by Troup and Berson (Berson, 1961; Troup, 1961; Berson and Troup, 1961) in the early 1960's and by Ramage (1971) later that decade. Troup studied the Australian monsoon at Darwin (12°26'S, 130°52'E) using data from six observation stations close to Darwin to define rain events. He showed that peak summer wet season events were accompanied by periods of moderate westerly winds at the surface. The work by Troup and co-workers were based on a limited upper air station network, and were intended to be order-of-magnitude calculations on the large scale mass, heat and momentum balances of the region. Most synoptic scale studies concentrated on local circulation features over Indonesia and/or northern Australia. During the late 1960's and early 1970's, the subject was largely neglected due to lack of data over the Southern Hemisphere summer monsoon domain (Murakami and Sumi, 1982a). Recently, as a consequence of the 1978-79 winter MONEX and the attention drawn to the El Niño/Southern Oscillation phenomena, there has been renewed interest in the world meteorological community on the Southern Hemisphere summer monsoon.

The summer monsoon of the Southern Hemisphere has many similarities with the northern summer monsoon over Southeast Asia and India. It is characterized by a monsoonal

equatorial trough in the lower troposphere, accompanied by low-level westerlies and upper-level easterlies (Ramage, 1971) which define the rotational wind components of the monsoonal circulation, and an abrupt poleward shift of the subtropical jet stream. The eastern end of the Southern Hemisphere monsoon trough (around 10°S, 170°E) is exemplified by a major low-level convergent center (850 mb) and an upper-level anticyclonic system (200 mb) associated with pronounced upper-level divergence (Murakami and Sumi, 1982a). A double Hadley cell structure occurs over the monsoon longitudes with the updraft center (ITCZ) lying along approximately 7°S. The latitudinal extent is more constrained than either the northern summer monsoon or the northern winter monsoon, extending poleward only along the Indonesian Islands, over Northern Australia and into the Solomon Sea with a large equatorward slope from the surface to the 850 mb level (Holland et.al., 1984). The longitudinal extent is denoted by a band of strong westerlies along about 10°S from the northeastern Indian Ocean (100°E), across the Indonesian Seas and New Guinea, to the western South Pacific Ocean (180°). The exact geographical extent is still unresolved.

Like the monsoons of the Northern Hemisphere, the southern summer monsoon also features active and break phases in monsoonal flow and convection. The summer monsoon's onset of an active phase is characterized by a step-like change in atmospheric circulation over the region. Low tropospheric westerlies and upper-level easterlies between the equator and 10°S strengthen dramatically. The Southern Hemisphere subtropical jet moves southward by more than 10°. The equatorial convergence zone moves south by several degrees, resulting in a large scale increase in the extent and intensity of tropical convection. This event has been extensively investigated by several authors (Davidson

et.al., 1983; Murakami and Sumi, 1982b). Its definition is of interest to this study since an objective means of determining the onset from the wind field is required in the subsequent analysis. The methods previously used to describe onset are based on conditions of enhanced activity in the winds and precipitation.

A number of methods have been proposed to define the onset of an active period of the Southern Hemisphere's summer monsoon. The fact that no method is generally accepted is due to marked regional differences in the behavior and timing of the onset over the domain of the Southern Hemisphere's summer monsoon. Consequently, there has been much discussion among meteorologists in the monsoon region as to the correct definition of onset. Troup (1961), for example, based his definition on two variables, wind and rainfall. By his wind criteria, the onset date is the beginning of the first spell of moderate west wind at the gradient level at Darwin. A spell of moderate west wind of N days duration is defined as a period when the cumulative zonal component exceeds $5.15 ms^{-1}$ for a time interval defined by (N+1) and is concluded when this component is less than $2.58 ms^{-1}$ on two consecutive days. Troup's rain criterion is based on daily observations at six stations close to Darwin. Onset is defined as the first occasion after 1 November on which four or more stations record rainfall and the area-averaged rainfall over N days exceeds 19.04mm for a time interval defined by (N+1).

Onset was objectively defined by Holland et.al. (1984) using the direction, strength and constancy of the low-level wind field (surface to 850 mb) over northern Australia. Davidson et.al. (1983) determined the onset date by subjectively analyzing satellite imagery for the first large-scale blow-up of tropical convection occurring over Australian longitudes. These criteria for blow-up required a span of

westerly subtropical jet stream which extends from northwestern Tibet to the central North Pacific Ocean at the 200 mb level. At 700 mb, the 200 mb features west of 120°E are replaced by the ridge over the Tibetian area which is probably the result of topographic effects. South of this anticyclone is another anticyclonic center over northern Australia with an easterly zonal flow over the maritime continent, separating the two centers.

Descending motion over Eurasia, in conjunction with ascending motion over the maritime continent, constitutes an overturning in a northwest to southeast plane. At the 200 mb level, the enhanced subsidence over northeast China and the increased tropical outflow over equatorial central Pacific Ocean are apparent in the east-west gradient of the isopleths. These two features are indicative of the strengthening of the east Asia local Hadley circulation and the two Walker circulations on either side of the maritime continent during winter. There are also secondary centers of convergence (divergence) off the west coast of South America and over northwestern South America, respectively.

The monthly mean ψ fields for the surface (Fig. 3.7) show the separation of the lower tropospheric midlatitude westerly regime and the tropical easterly regime by a strong subtropical ridge. Note that maxima (minima) in the North (South) Hemisphere are indicated by solid (dashed) lines. The Mongolian high, with its clearly defined northwest to southeast orientation, intensifies through the winter, indicating a penetration of midlatitude air into the tropics along the east coast of China. This implies that the increased northeasterly winds are primarily due to the rotational part of the wind. During the same period, the Western Australian low intensifies and the vorticity trough expands, migrating southward toward the equator until it encompasses the maritime continent region.

At the 700 and 200 mb levels (Figs. 3.8 and 3.9), the most outstanding feature is the presence of a prominent east-west oriented anticyclone, centered at approximately 25°N, 162°E, which encompasses the entire subtropical Pacific, as well as, extending in an elongated fashion eastward to the central North Pacific Ocean and westward to eastern Africa at the 200 mb level. This anticyclone is separated from a cyclonic center to the north by the

The primary divergence zone at the surface is located over China and Mongolia with a northwest to southeast tilt. It has two maxima, one over the east coast of China and the other over Mongolia, just southwest of Lake Baikal (45°N, 93°E). This second maxima may actually be located slightly to the north by a few degrees, because the artificial boundary conditions imposed may influence the region within about 10° from the boundary. Secondary regions of divergence are found in the southern Indian Ocean and in the eastern areas of the North and South Pacific Oceans.

December and January show some intensification in the north-south gradient of the X isopleths between the equatorial convergence and the East China coast divergence maxima between 100°-140°E. This is indicative of the lower branch of the local East Asia Hadley cell.

The 700 mb X field (Fig. 3.5) clearly delineates the SPCZ centered on the equator from the Celebes Sea to the central South Pacific Ocean with a west-southwest to east-northeast orientation that is consistent with the OLR pattern seen in Boyle and Lau (1984). This convergence zone, although distinctly weaker than at the surface, expands and intensifies throughout the season. This zone of convergence is clearly much deeper than the low-level convergence zones over Brazil, the Indian Ocean, and equatorial Africa which are not evident at the 700 mb level. In comparison, the data of Oort (1983) shows a sharp reduction in the magnitude of the divergence over the African and South American convection centers when going from the surface to the 700 mb level but it is not as great as indicated by Fig. 3.5. To the north and east, broad scale divergence exists over Mongolia and the equatorial and central Pacific Ocean.

The 200 mb monthly mean X fields (Fig. 3.6), coupled with the mean fields of the lower levels, present an overview of the three-dimensional planetary-scale circulation.

B. VELOCITY POTENTIAL AND STREAMFUNCTION

To provide a horizontal and vertical perspective of the rotational and divergent components in tropical-midlatitude interactions, the time mean charts of velocity potential and streamfunction were examined. As pointed out by Chang and Lau (1980) and Davidson (1984), changes in convection may often be inferred from variations in the divergent wind. From equation 2.3, it can be seen that maxima (minima) in values of χ correspond to divergence (convergence) centers. The sense of divergent flow is from high to low χ values and its strength is proportional to $\nabla\chi$. Thus, one can infer that at lower (upper) levels, convergence (divergence) represents large scale rising motion. The rotational aspects of the flow are imparted by variations in the streamfunction. Maxima (minima) of ψ in the Northern (Southern) Hemisphere correspond to centers of anticyclonic flow (equation 2.2).

The monthly mean χ field for the surface (Fig. 3.4) shows a broad region of convergence in the equatorial region between 10°S and 10°N from the central Indian Ocean to the mid-Pacific Ocean. The zone of convergence maximum is centered over the equator in November and December. It expands in January and Febuary and migrates south of the equator to lay over northern Australia and New Guinea. This maximum surface convergence zone is basically oriented in an east-west direction which is different from the west-southwest to east-northeast tilt of the South Pacific Convergence Zone (SPCZ) cloudiness evident in monthly mean charts of outgoing longwave radiation (OLR), Boyle and Lau, (1984). There is also a secondary maximum over the northern portion of South America. In general, the surface convergence centers correspond well with minima in the tropical CLR fields.

feature in the South China Sea. This is evidence of the intense baroclinity present in the region. Embedded in the wide midlatitude westerly flow, the subtropical jet stream has its maximum farther west than the maximum at 200 mb (Fig. 3.3), indicating a possible upstream topographic influence due to the Tibetian plateau. The winds in the Indonesia-Arafura Sea region are easterly. There is no evidence of the western Australian low-level cyclone that is observed at the surface, consistent with heat low structure. It has been replaced by a weak ill-formed anticyclone which becomes stronger from December to February, migrating to central Australia.

Some flow field characteristics of the low-level do persist to the 700 mb level. The surface Mongolian high endures as a broad scale ridge. The subtropical ridge (25°N) remains while cross equatorial flow appears as a slight feature in January. The easterly trade region, equatorward of the subtropical ridge, expands eastward across the Pacific Ocean, crossing the equator in February.

The 200 mb level (Fig. 3.3) is dominated by strong midlatitude westerly flow regimes in both Northern and Southern Hemispheres. The Northern Hemispheric flow is characterized with a maximum of the subtropical jet (>50-70 ms^{-1}) centered over Japan which exhibits a west-southwest to east-northeast orientation in early winter. The wind maximum in November (>30 ms^{-1}) over central Australia, which extends into the central South Pacific Ocean, weakens in December. Generally weak easterly flow is found in the tropical latitudes of the Indian Ocean, maritime continent and Western Pacific Ocean, and South America, although an enhanced region of easterlies migrates into the vicinity of the maritime continent in December and expands in January. A permanent anticyclonic gyre is found in central South America and southern Africa.

south of the equator (5°-10°S) in December. In the general vicinity of the Indonesia-Arafura Sea region, the equatorial zonal wind along 10°S is generally weak in November but develops into westerlies which expand eastward from December to February. This is an important indicator of the Indonesian monsoon which we will use to study the possible relationship between the northern winds and the southern summer monsoons. In conjunction with these monsoonal westerlies, an area of persistent cyclonic shear exists in the northeast portion of Australia. Strong southerly winds along Australia's west coast corresponds to the location of the heat low described by Ramage (1971, p15).

Other features of note within both hemispheres include the Mongolian high, the northern subtropical ridge along 25°N, and the South Pacific Ocean easterlies. The Mongolian anticyclone (50°N, 93°E) is established by November as a persistent feature and intensifies in December and January. The basic low-level flow in the region of central China and east China coast are westerlies north of this high center, becoming weak northerlies in the East China Sea and northeasterly through the South China Sea to the Malaysian Peninsula. To the east, an extensive subtropical ridge persists across the central North Pacific Ocean along 25°N, separating the midlatitude westerlies from the northeast trades on the equatorward side. The northeast trades range over the entire tropical region of the North Pacific Ocean. Cross equatorial flow is weak in November and December but strengthens slightly and expands across the Pacific Ocean in January and February. Easterlies dominate the central South Pacific Ocean with a wind maximum extending from the west coast of South America.

At the 700 mb level (Fig. 3.2), the key circulation features discussed above have either dissipated or reversed. The northeasterly monsoonal flow has been replaced by predominantly westerly winds although it remains as a slight

III. TIME MEAN CIRCULATION

Nine-year (1974-1983) monthly mean circulation fields at 200 mb, 700 mb and the surface were calculated for the months of November, December, January and February. The variables are wind, velocity potential and streamfunction.

A. WIND

The three key circulation features germane to this study, i.e., the surface northeast monsoonal winds in the South China Sea, the zonal winds along 10°S and the western Australian trough, are clearly seen in the surface wind (Fig. 3.1). The northeast monsoon regime is already in place in November with a maximum ($>10 ms^{-1}$) in the northern region of the South China Sea. In December, the monscon winds strengthen and the northeast-southwest oriented isotach maximum becomes more extended, connecting the middle and high latitude regions of northeast Asia and Japan with the equatorial South China Sea. Elsewhere the global tropics are covered by the surface northeast trades equatorward of the subtropical ridge. The narrow band of the East Asian winter monsoon winds over the South China Sea stands out distinctly as the only regime where the north-northeasterlies extend from the tropics to middle latitudes. This is quite suggestive of a midlatitude-tropical interaction within this region. Although the isotach maximum weakens somewhat in January and February, the pattern persists throughout the season.

In November and December, the equatorial trough is ill-organized but becomes well defined in January. A confluence zone is centered over the equator in November but migrates

that their values are not excessively affected by the choice of boundary conditions.

The data base was carefully reviewed to identify missing or erroneous fields. The end result yielded few data gaps. The only significant block of missing data runs from 1200GMT 06 December 1976 to 1200GMT 16 December 1976. Inconsistent or missing data were replaced by linearly interpolated values based on the closest adjacent data.

To study the possible relationship between the northern winter monsoon winds and the southern equatorial monsoons winds, the following analyzed data were produced:

1. monthly means of the observed wind, streamfunction, and velocity potential for the surface, 700 and 200 mb levels for the nine winters.

2. area averaged parameters of wind and vorticity whose time variations represent certain circulation features of the monsoons.

3. composited area averaged parameters and composited surface wind field for periods of pre- and post-onset of the acceleration of the Indonesian equatorial zonal winds.

Here the streamfunction ψ and the velocity potential χ are obtained trough the Poisson equations

$$\nabla^2 \psi = \zeta = \left(\frac{\partial v}{\partial x} - \frac{\partial u \cos\phi}{\cos\phi \, \partial y} \right) \sec\phi \qquad (2.2)$$

$$\nabla^2 \chi = -\delta = -\left(\frac{\partial u}{\partial x} + \frac{\partial v \cos\phi}{\cos\phi \, \partial y} \right) \sec\phi \qquad (2.3)$$

where ζ is the relative vorticity

$$\frac{\partial v}{\partial y} - \frac{\partial u}{\partial x} \qquad (2.4)$$

and δ is the divergence

$$\frac{\partial u}{\partial x} + \frac{\partial v}{\partial y} . \qquad (2.5)$$

The horizontal coordinates in the Mercator projection are defined as:

$$x = a\lambda , \quad y = a \ln\left(\frac{1 + \sin\phi}{\cos\phi} \right) . \qquad (2.6)$$

where a is the radius of the earth, and λ and ϕ are longitude and latitude, respectively. Both ζ and δ were approximated using centered differences on the GBA Mercator grid.

In solving equation 2.3, it was assumed that $\chi = 0$ at the north and south boundaries of 60°N and 40°S, respectively. The technique used to calculate ψ was essentially method II of Shukla and Saha (1974). This method uses the previously computed χ field to formulate boundary conditions for ψ . The values of ψ are displayed above 50°N although the solution for ψ encountered at this boundary is difficult due to this region being meteorologically active. It is assumed that the χ and ψ fields in the equatorial regions are sufficiently removed from the boundaries such

II. DATA AND PROCEDURE

The wind data set used in this study is based on the operational Global Band Analysis (GBA) of the United States Navy's Fleet Numerical Oceanography Center (FNOC). This analysis is available twice daily by objective procedures on a 49 x 144 Mercator grid extending from 40°S to 60°N around the tropical belt. The Mercator secant projection results in a change in the actual distance between grid points from 140 km at 60°N to a maximum value of 280 km at the equator. The objective scheme takes advantage of all reports in the operational data base: surface synoptic, aircraft, pilot balloons, rawinsonde and satellite data. Using the six-hour persistence field as the first guess, irregularly spaced data are first interpolated to grid points using the successive corrections technique based on Cressman's (1959) method. The successive corrections method takes several scans through the data, reducing the radius of the influence of the observations on each successive scan. These fields are then adjusted by a set of numerical variation analysis (NVA) equations which incorporate the dynamic constraints of the momentum equations, with friction included in the surface layer (Lewis and Grayson, 1972).

The period of study is the nine Northern Hemisphere winter monsoon seasons (November-February) of 1974-75 through 1982-83. The levels of interest are the surface, 700 mb, 400 mb, and 200 mb zonal (u) and meridional (v) velocity components. These components are subsequently divided into rotational and divergent parts, i.e.,

$$V = \nabla \chi + k \times \nabla \psi \qquad (2.1)$$

Its significance as a key parameter lies in the fact that monsoonal westerlies, as defined by Troup(1961) and Davidson et.al. (1983), are the precursor to monsoonal rainfall over northern Australia. In this study, the correspondence of changes in this parameter with other circulation feature parameters is reviewed to investigate any possible interhemispheric influences.

4. Surge of Low Level Southerly Winds along the Western Australian Coast. Prior to onset, a surge of low-level southerly winds parallel the western Australian coastline. These surges have been linked physically to the intensity of Indian Ocean anticyclones and the passage of frontal systems past the southwest corner of the Australian continent. Their significance in triggering monsoon convection may be an important component in the Southern Hemisphere midlatitude interaction with the tropics (Davidson et.al., 1983).

The purpose of this study is to identify the possible influences of the northeast monsoon in the Northern Hemisphere on the Southern Hemisphere's summer monsoon. A valuable concurrent work to study the internemispheric interactions was the construction of a nine-year montnly mean climatology of the global wind field from 60°N to 40°S at the surface, 700 and 200 mb levels. The acceleration of the scuthern equatorial zonal wind along 10°S will be used as the main parameter to represent the onset of the southern summer monsoon. There are two reasons for choosing this parameter instead of rainfall or satellite imagery. First, the variation of the northern winter monsoon is best represented by the surface northeast winds and it is anticipated that the signal of its possible influences may be more apparent in the surface winds of the southern summer monsoon. Second, among all southern summer monsoon indicators ccmmonly used, these low-level equatorial westerlies are the closest to the equator and, therefore, should be the first indicator to show any influence from the Northern Hemisphere. This acceleration parameter is only applicable to the monsoonal winds in the Indonesia-Arafura Sea region and may not describe other features of the complete Southern Hemisphere's summer mcnsoon with a one-to-one relationship.

circulation was forced primarily by differential heating of land and ocean due to changing seasonal radiation inputs. Thus, temperature gradients have developed to a state where the troposphere is ready for onset to occur.

2. Westward Expansion of Monsoon Westerlies. The proposal by Murakami and Sumi (1982b), based on data collected during the Winter Monsoon Experiment (WMONEX) of December 1978 to February 1979, suggested that monsoonal onset was initiated by events occurring away from the Indonesia-Arafura Sea region. Due to northeasterly trade wind intensification over the tropical North Pacific Ocean, cross equatorial northwesterlies result near 170°E. This induces a zone of strong westerlies which expand westward into the Indonesia-Arafura Sea region and establishes the monsoon.

3. Cold Surges in the South China Sea. It has been hypothesized that northeastly cold surges in the South China Sea influence the triggering of summer monsoonal onset. Lim and Chang (1981) used linearized shallow-water equations on an equatorial β plane to demonstrate the dynamic response of the tropical atmosphere to midlatitude pressure surges. They showed that such baroclinic surges in the Northern Hemisphere midlatitudes induce pressure rises at the equator and low latitude cyclone development in the region of the Southern Hemisphere equatorial trough. This implies that northeast monsoon surges in the Northern Hemisphere could induce a response in the southern tropics that contains certain aspects of the southern summer monsoon.

10° latitude by more than 30° longitude of cloud cover which persists for several days. A comparison between dates given by Troup's wind definition and those determined subjectively from satellite imagery by Davidson et.al., (1983) found the dates to be within five days of each other. Poor correspondence was found with Troup's rain onset criterion. Closer to the equator, the Indonesian meteorologists define the onset based on the reversal of surface winds from easterly to westerly. Rain is often associated with westerly monsoonal wind. By any criterion, southern summer monsoon onset typically occurs between mid-December and mid-January.

Many hypothesis and theories have been presented to explain the triggering mechanisms for the onset of an active monsoon period in the Indonesia-Arafura Sea region. Of these, the main propcsals are:

1. Southern Hemisphere's Tropical-Midlatitude Interactions. Davidson et.al. (1983) postulated that changes, occurring prior to the onset of the southern summer monsoon, take place in the large scale flow of the subtropics south of the monsoon region. The synoptic situation leading to onset is typified by a subtropical ridge, extending over the southwest corner of Australia, which is disrupted by a trough stretching westward into the low latitudes. This trough also causes the monsoon shear line to be interrupted. Subsequently, the trough migrates eastward permitting anticyclogenesis in southern Australia, which persists until tropical convection is enhanced and onset occurs. Thus, convection and monsoonal onset occur after a period of anticyclogenesis and is triggered by the developement of a succession of high-low pressure systems and their movement within the subtropics. They hypothesized that this monsoonal

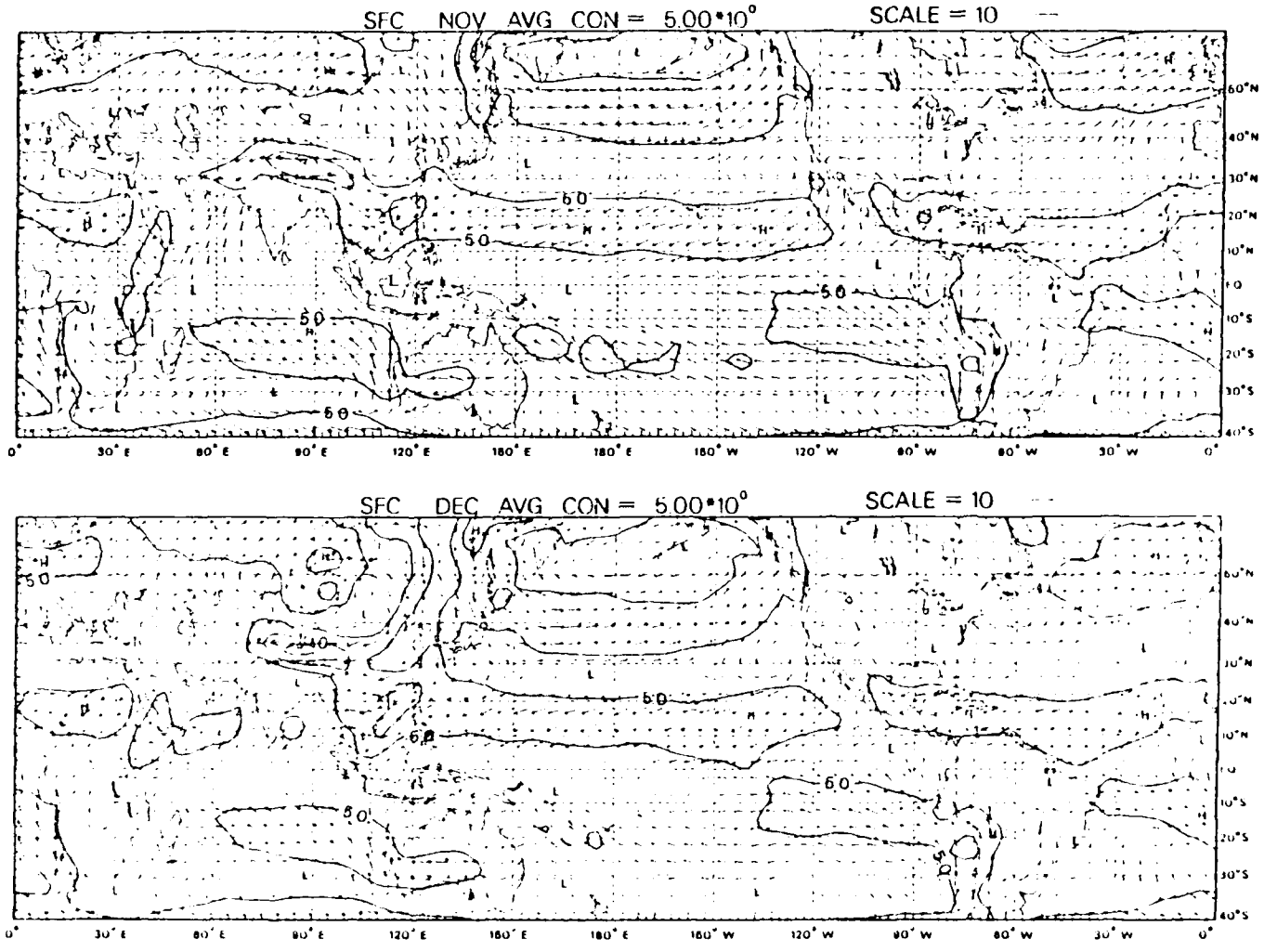

Fig. 3.1 Latitude-longitude sections of nine-year monthly mean surface wind vectors and isotachs.

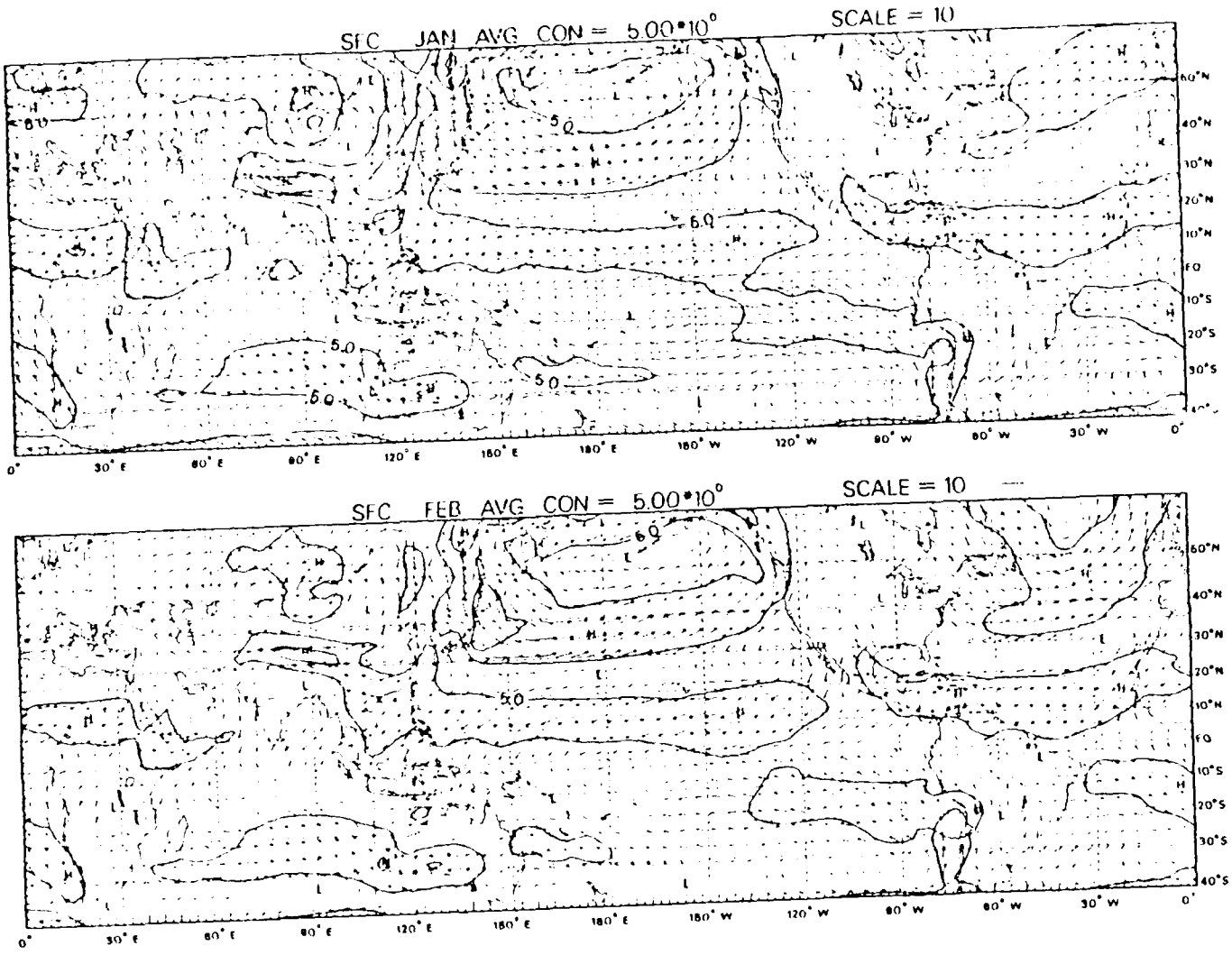

Fig. 3.1 (cont'd.)

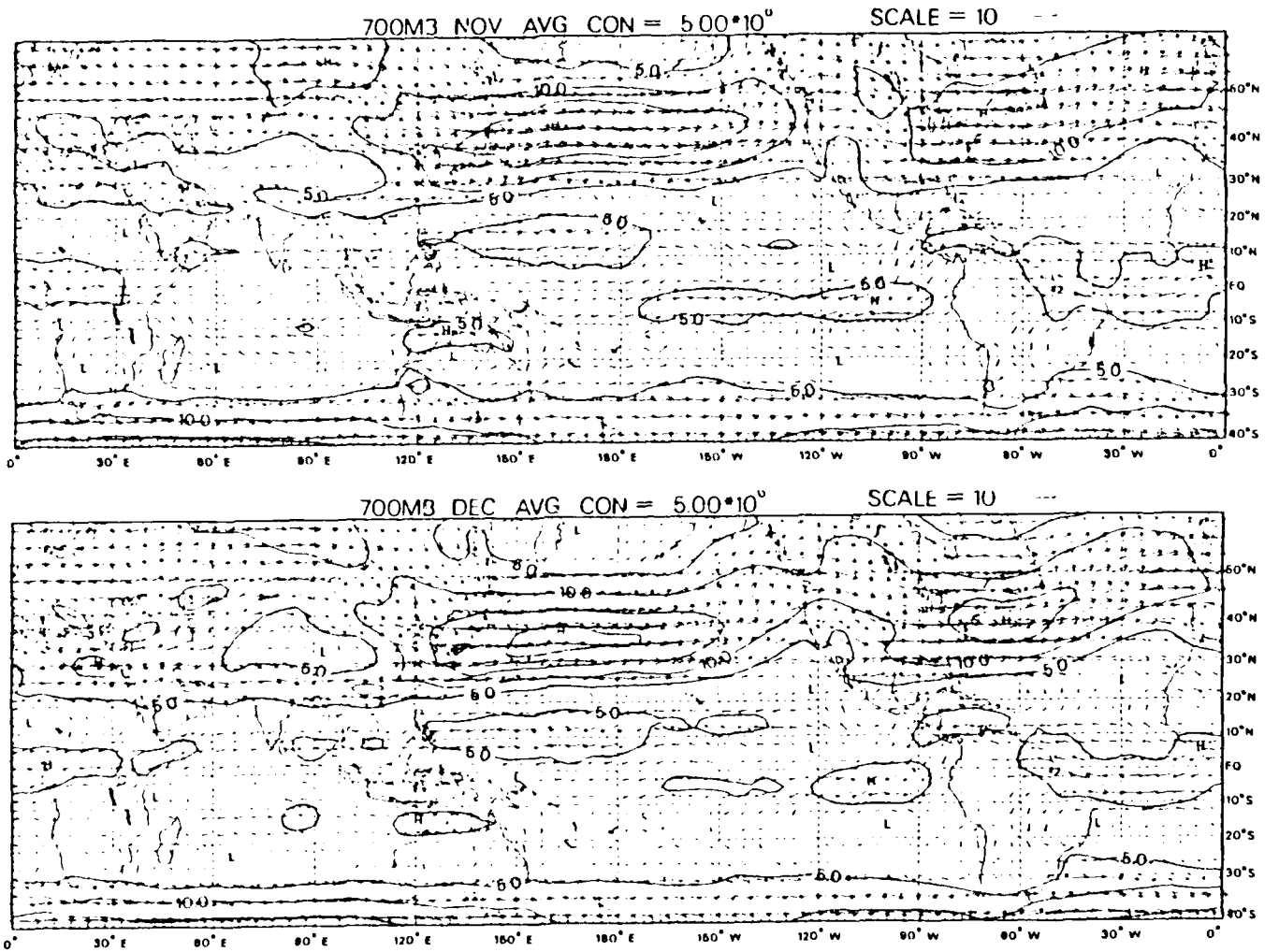

Fig. 3.2 As in Fig. 3.1, except for 700 mb level.

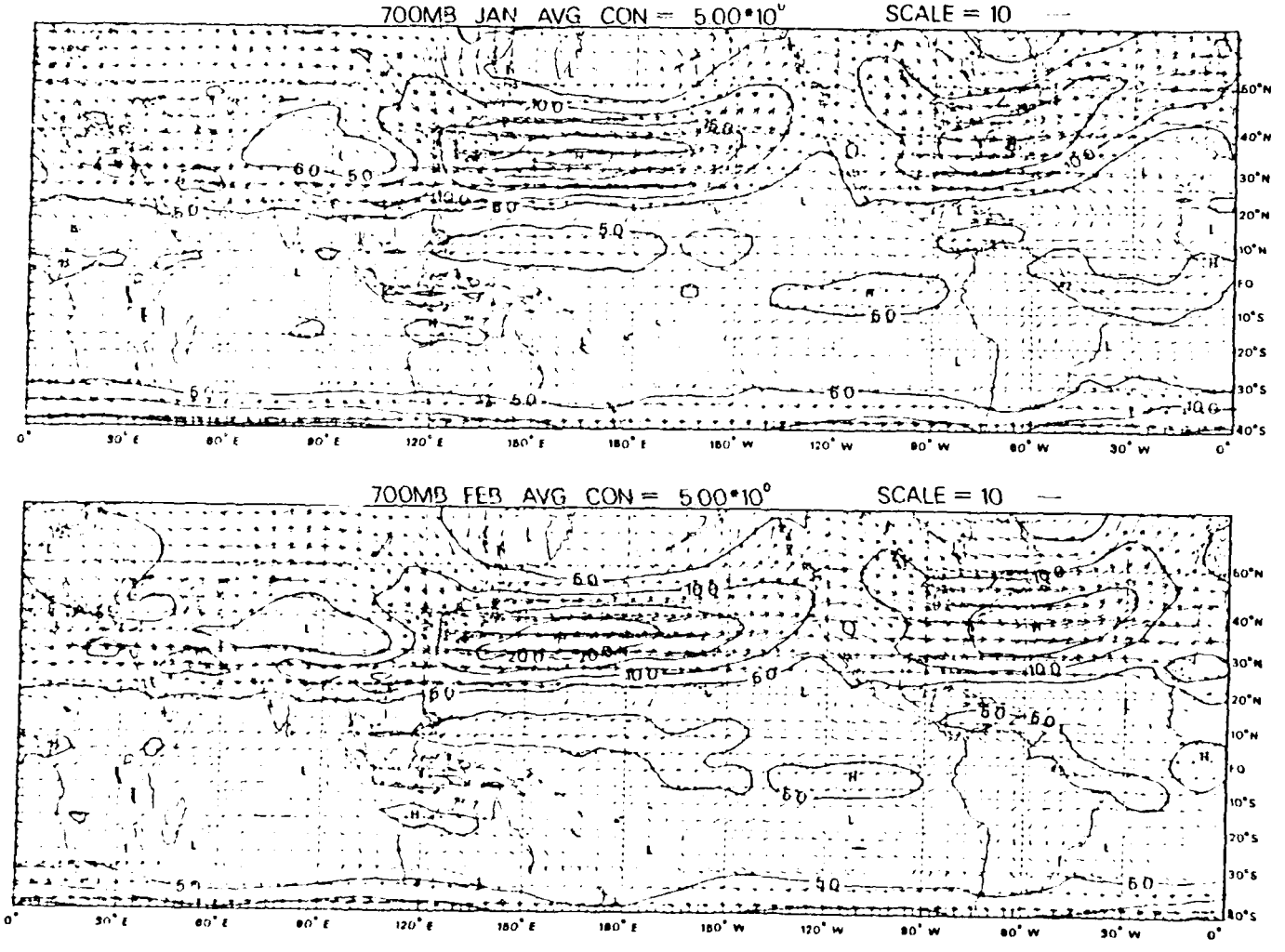
700MB JAN AVG CON = 500*10
SCALE = 10
700MB FEB AVG CON = 500*10
SCALE = 10

Fig. 3.2 (cont'd.)

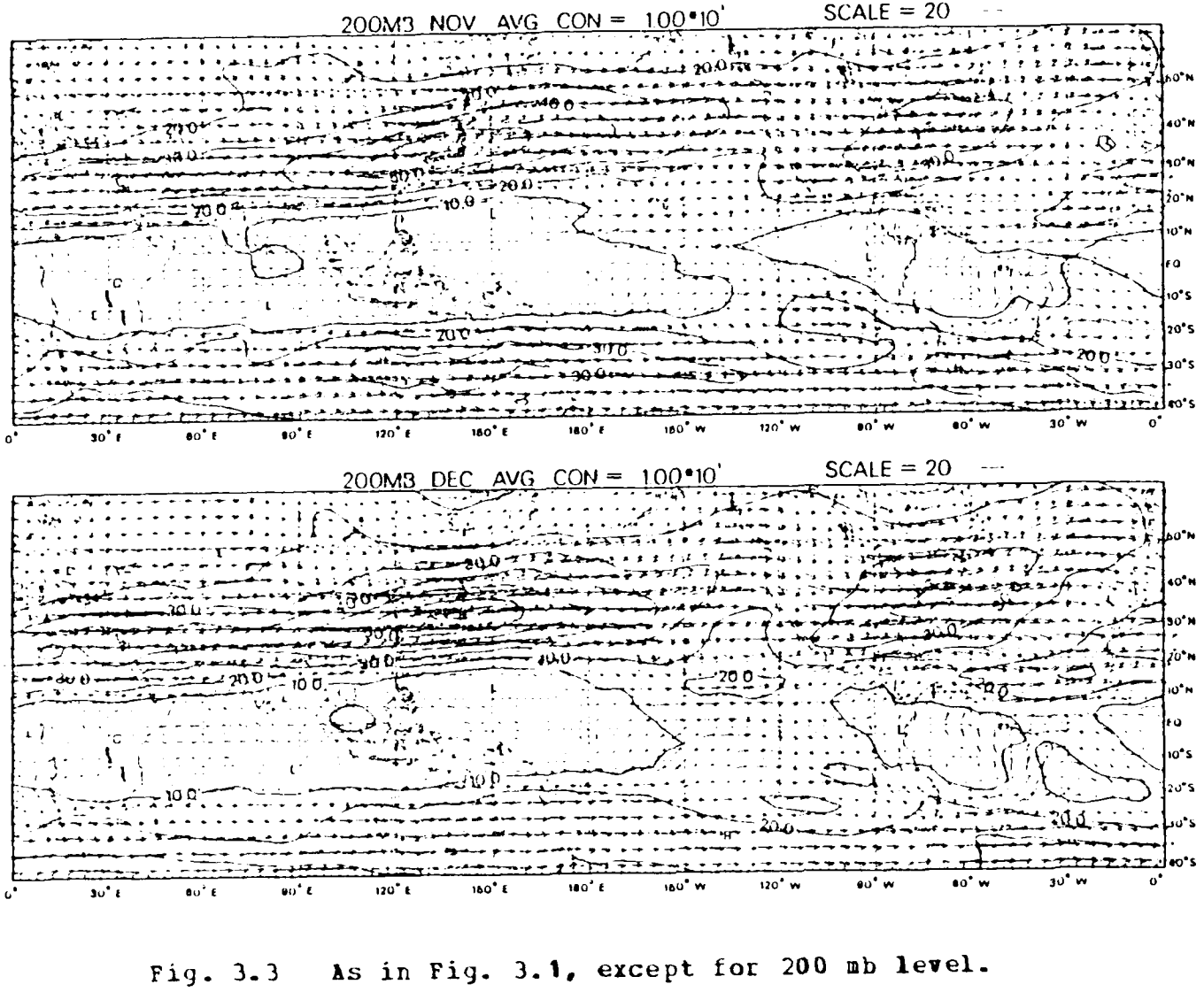

Fig. 3.3 As in Fig. 3.1, except for 200 mb level.

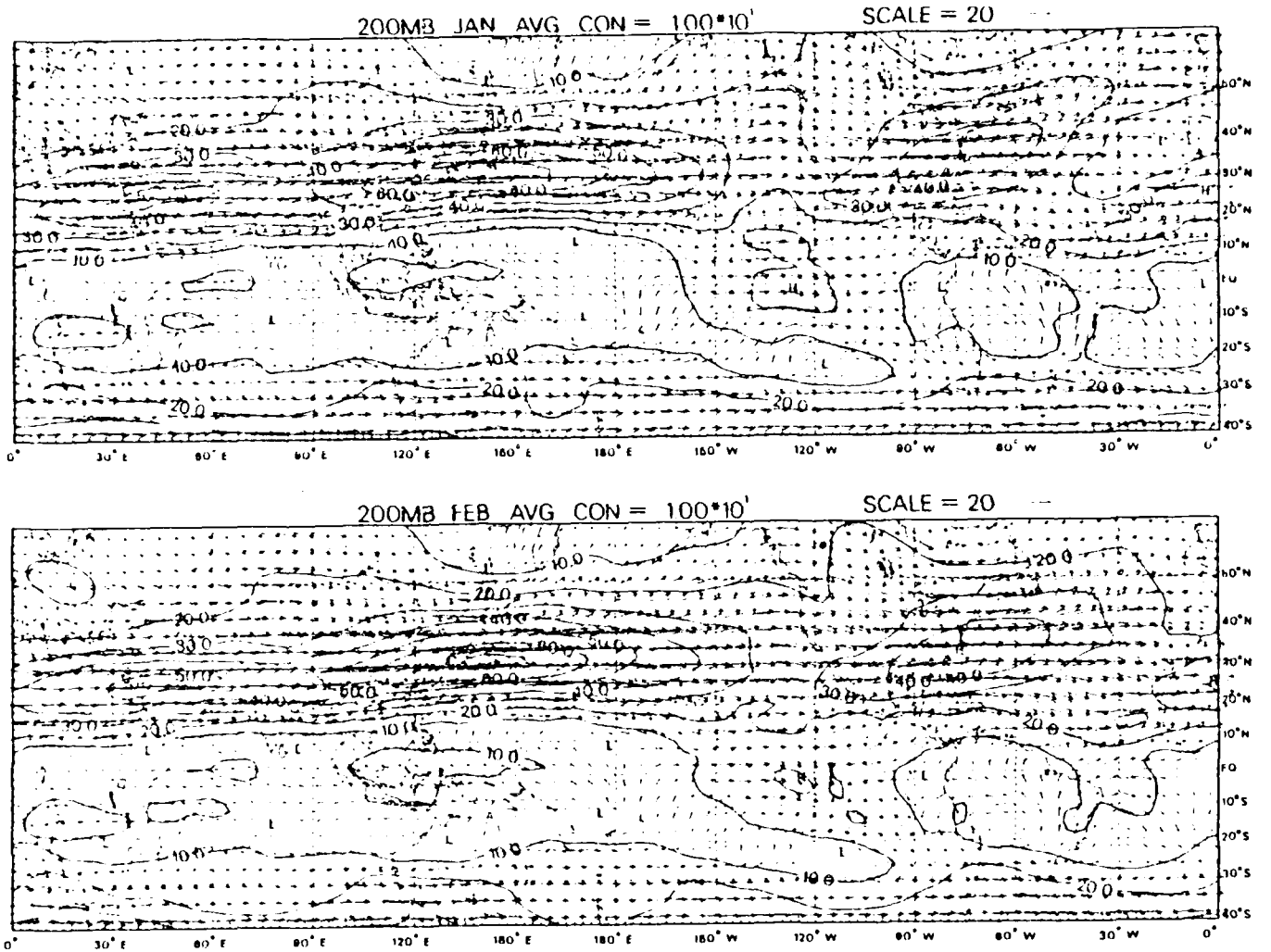
200MB JAN AVG CON = 100*10'
SCALE = 20
200MB FEB AVG CON = 100*10'
SCALE = 20

Fig. 3.3 (cont'd.)

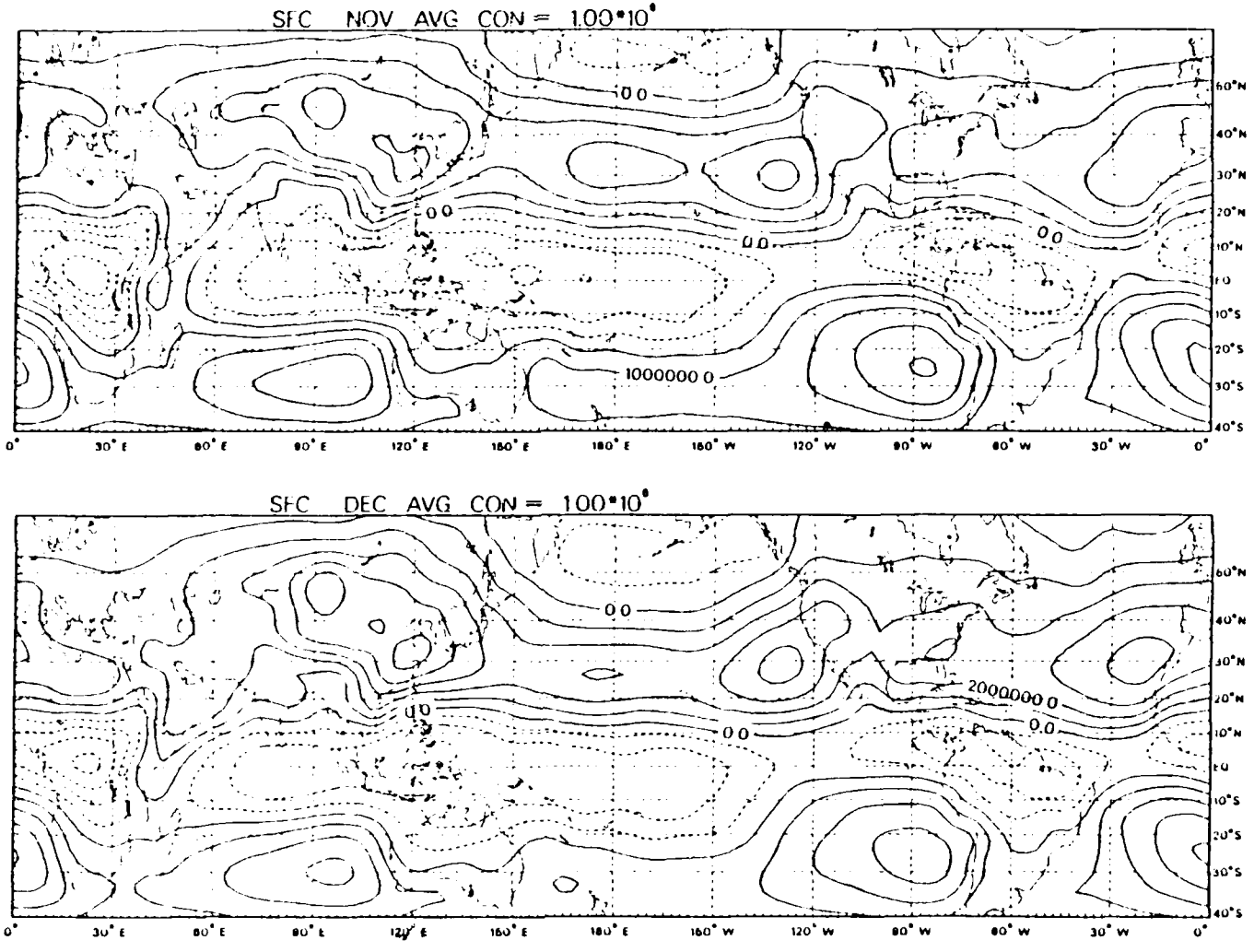

Fig. 3.4 Latitude-longitude sections of nine-year monthly mean surface velocity potential. Positive(zero) values are solid.

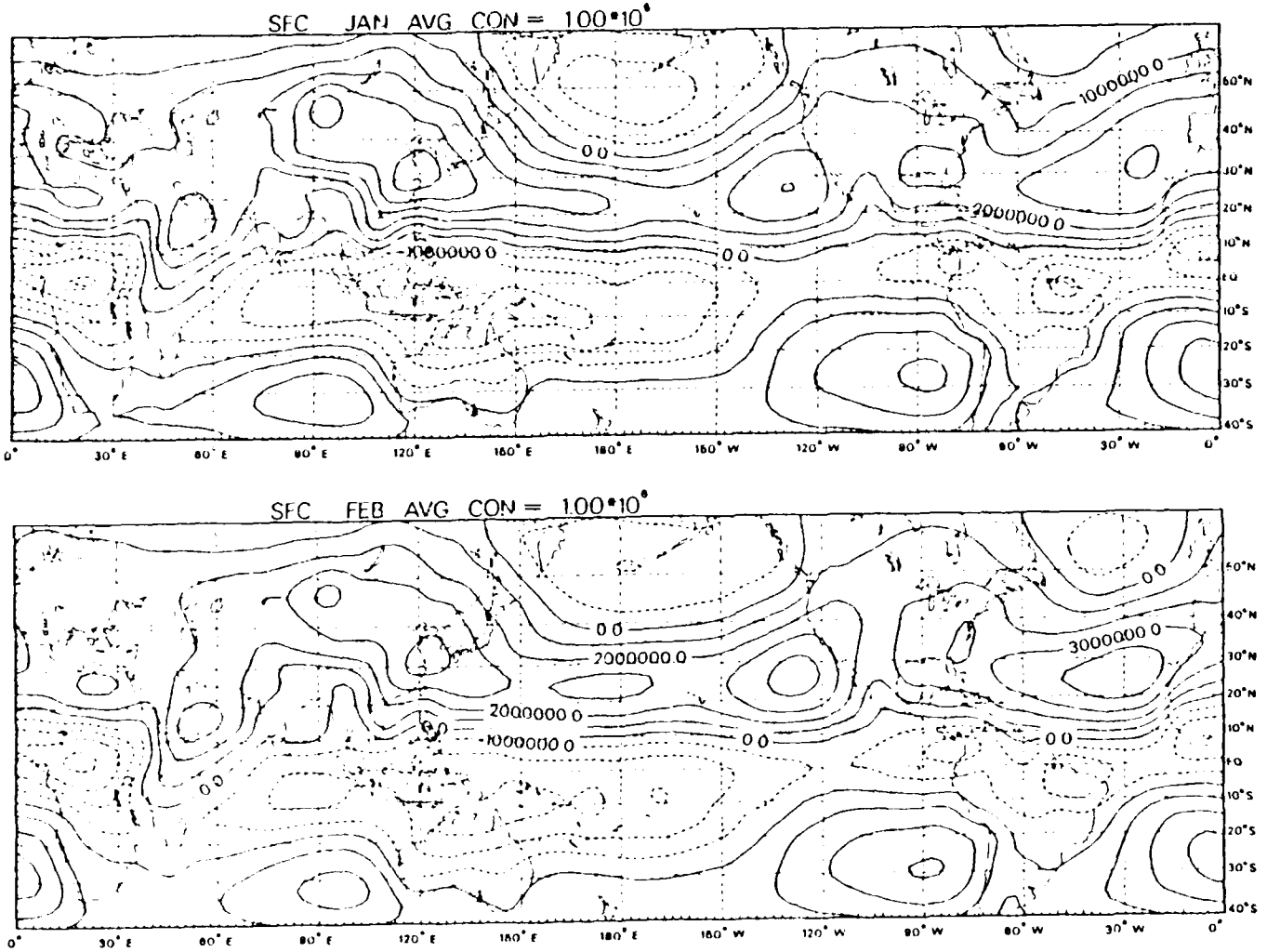
SFC JAN AVG CON = 100*10⁶
1000000 0
0 0
2000000 0
-1000000 0
0 0
60°N
40°N
30°N
20°N
10°N
EQ
10°S
20°S
30°S
40°S
0°
30° E
60° E
90° E
120° E
150° E
180° E
150° W
120° W
90° W
60° W
30° W
0°
SFC FEB AVG CON = 100*10⁶
0 0
2000000 0
3000000 0
2000000 0
-1000000 0
0 0
0 0
0 0
60°N
40°N
30°N
20°N
10°N
EQ
10°S
20°S
30°S
40°S
0°
30° E
60° E
90° E
120° E
150° E
180° E
150° W
120° W
90° W
60° W
30° W
0°

Fig. 3.4 (cont'd.)

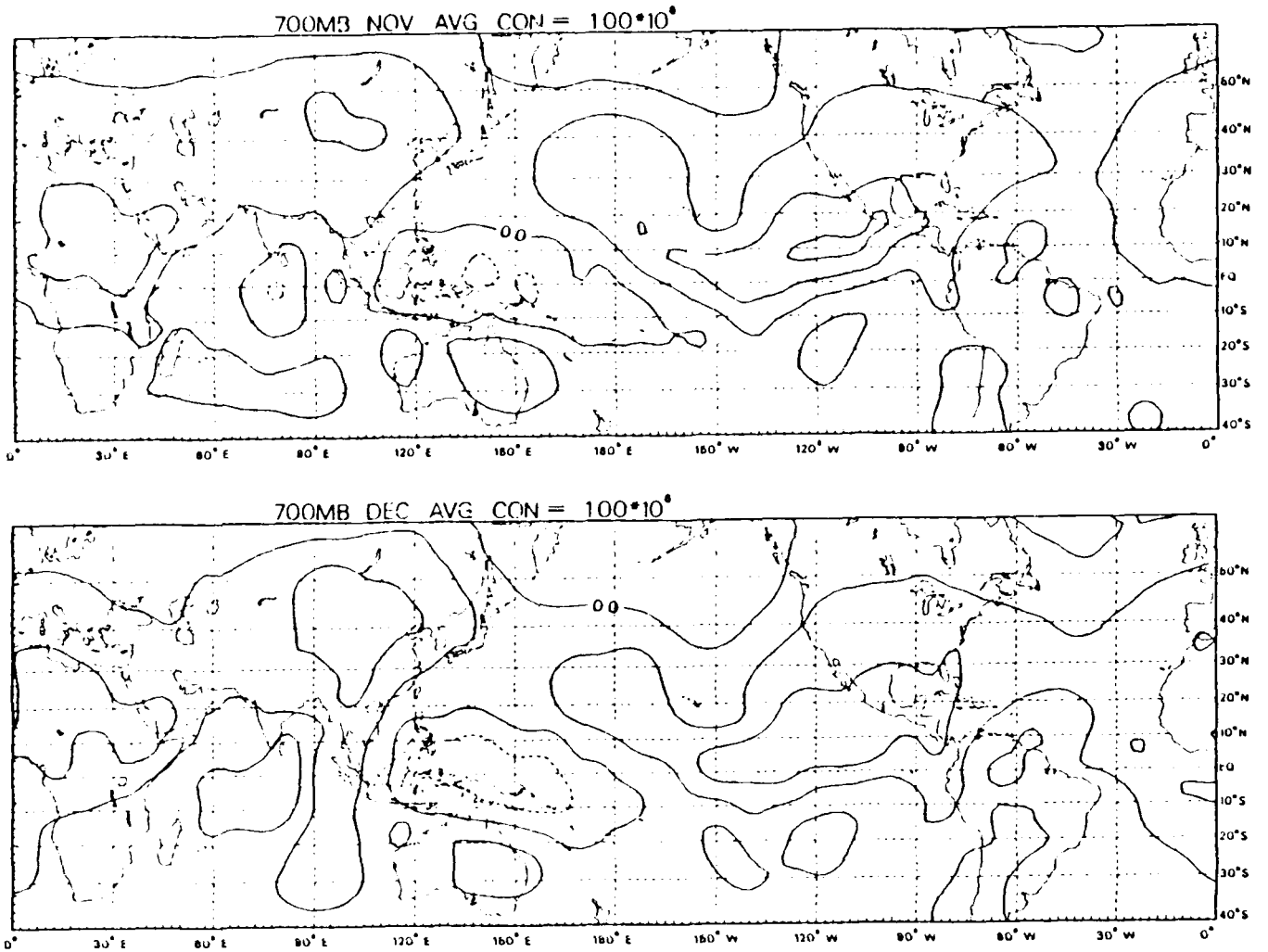

Fig. 3.5 As in Fig. 3.4, except for 700 mb level.

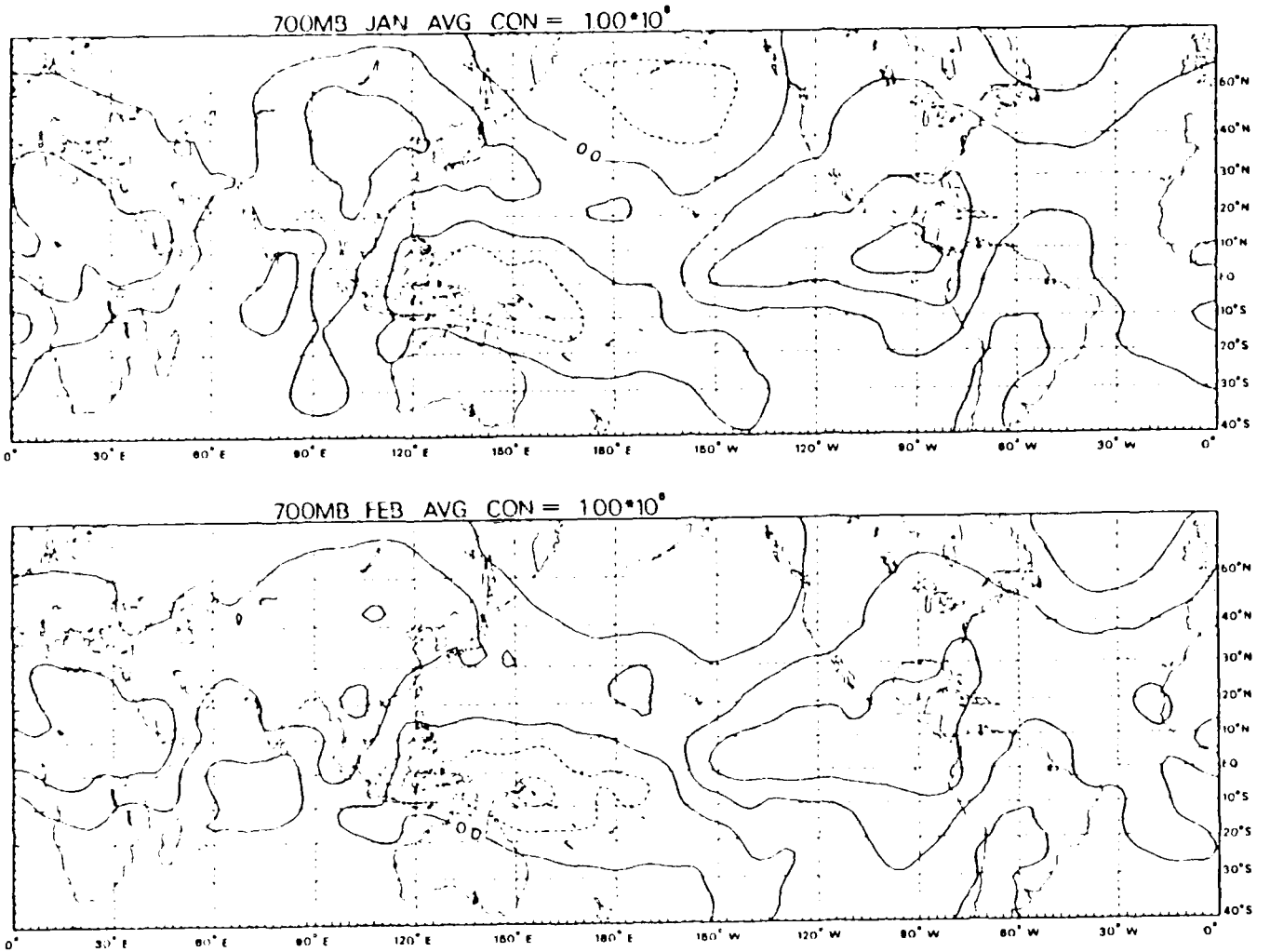
700MB JAN AVG CON = 100*10⁶
60°N
40°N
30°N
20°N
10°N
EQ
10°S
20°S
30°S
40°S
0°
30° E
60° E
90° E
120° E
150° E
180° E
150° W
120° W
90° W
60° W
30° W
0°
700MB FEB AVG CON = 100*10⁶
60°N
40°N
30°N
20°N
10°N
EQ
10°S
20°S
30°S
40°S
0°
30° E
60° E
90° E
120° E
150° E
180° E
150° W
120° W
90° W
60° W
30° W
0°

Fig. 3.5 (cont'd.)

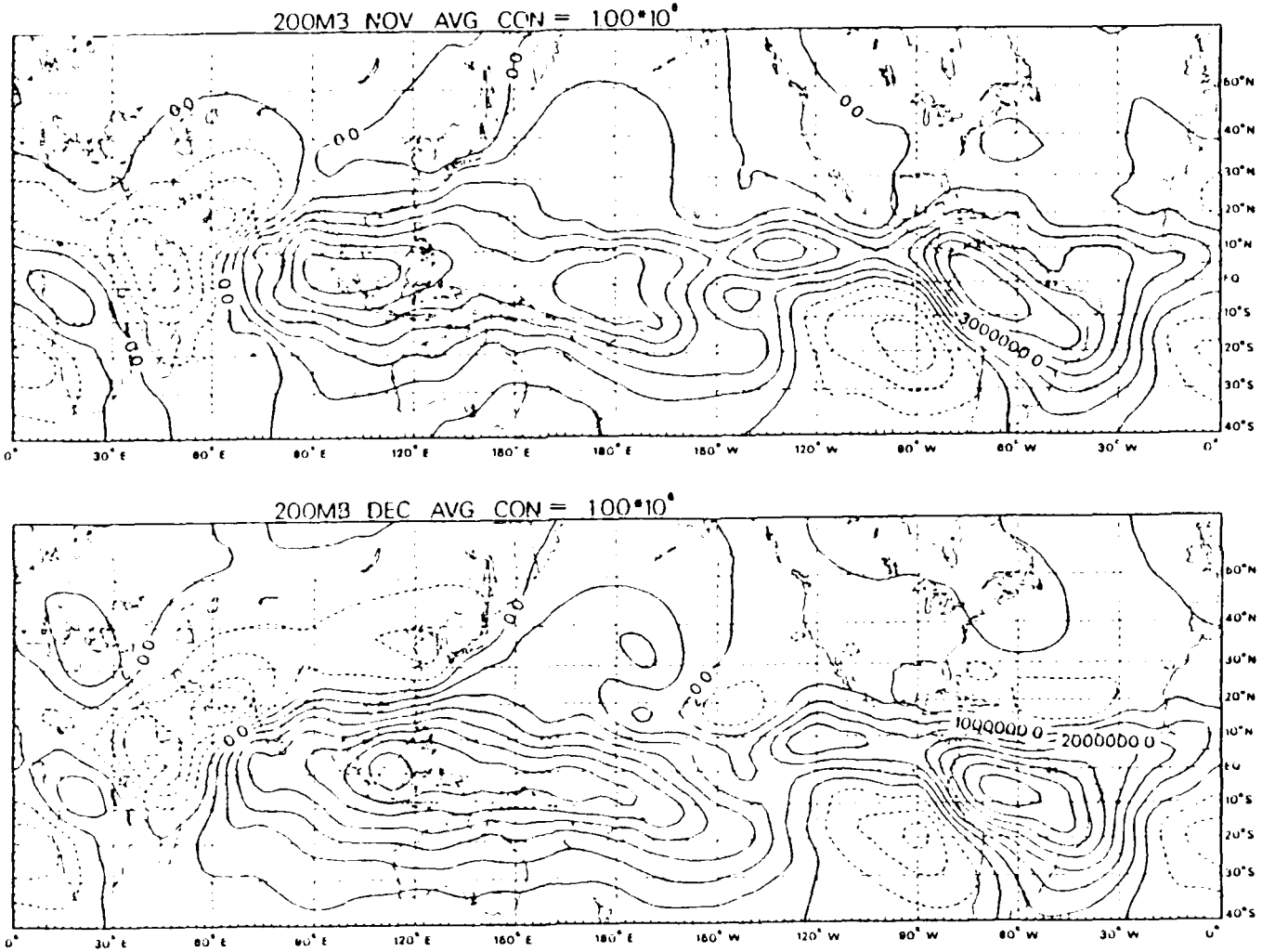

Fig. 3.6 As in Fig. 3.4, except for 200 mb level.

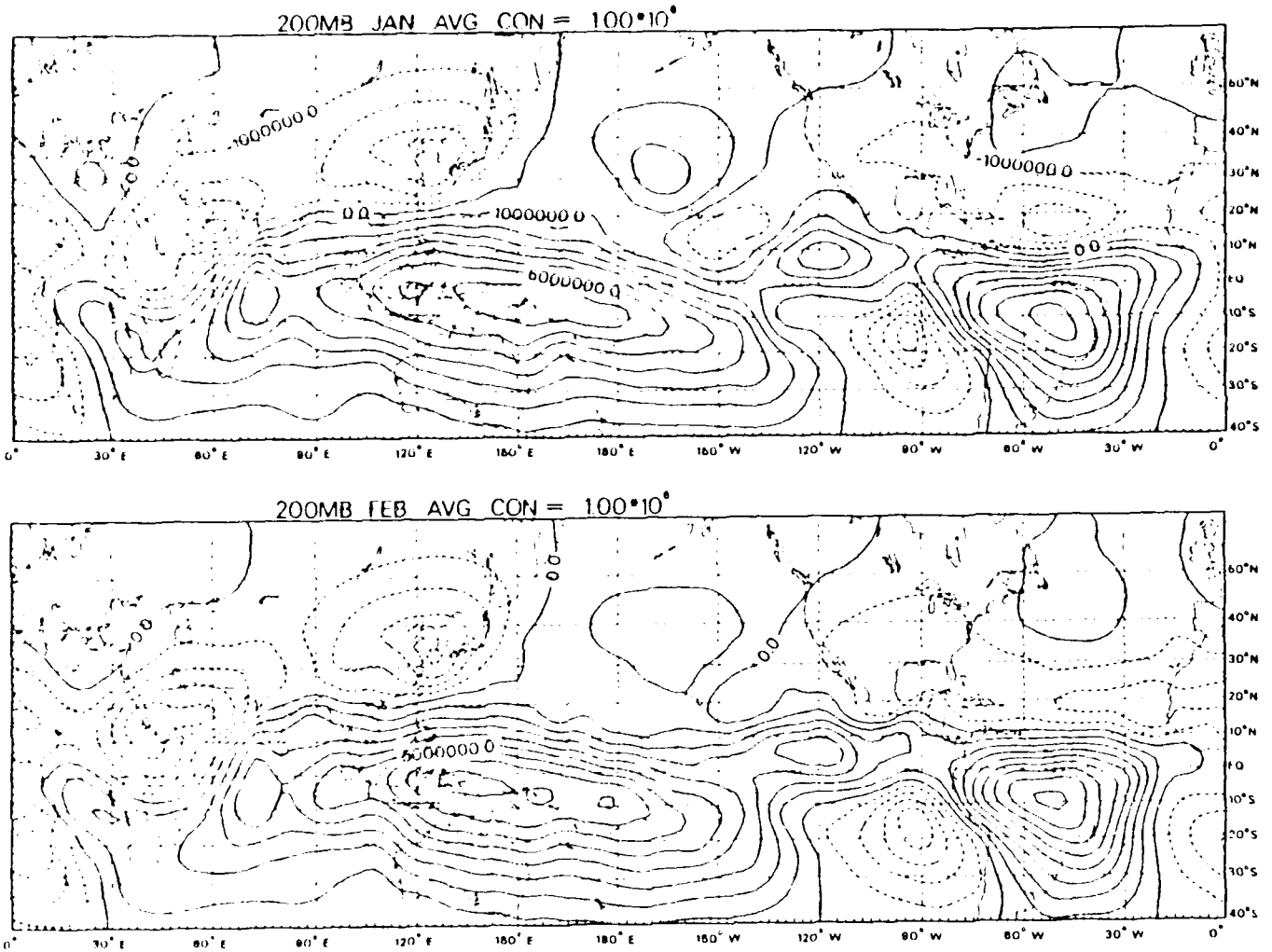
200MB JAN AVG CON = 100*10⁶
1000000.0
1000000.0
1000000.0
6000000.0
0.0
0.0
60°N
40°N
30°N
20°N
10°N
EQ
10°S
20°S
30°S
40°S
0°
30° E
60° E
90° E
120° E
150° E
180° E
150° W
120° W
90° W
60° W
30° W
0°
200MB FEB AVG CON = 100*10⁶
6000000.0
0.0
0.0
60°N
40°N
30°N
20°N
10°N
EQ
10°S
20°S
30°S
40°S
0°
30° E
60° E
90° E
120° E
150° E
180° E
150° W
120° W
90° W
60° W
30° W
0°

Fig. 3.6 (cont'd.)

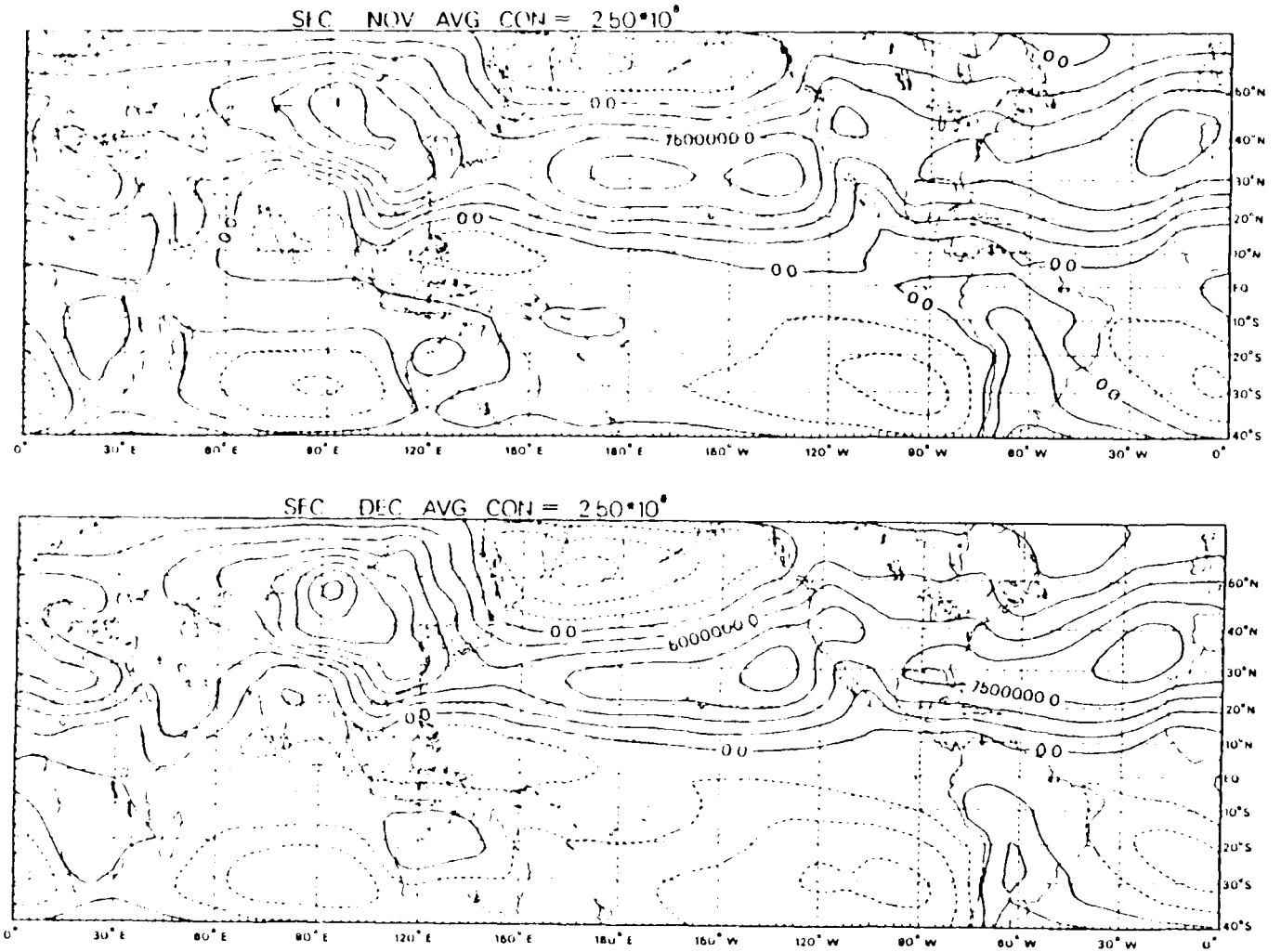

Fig. 3.7 Latitude-longitude sections of nine-year monthly mean surface streamfunction.

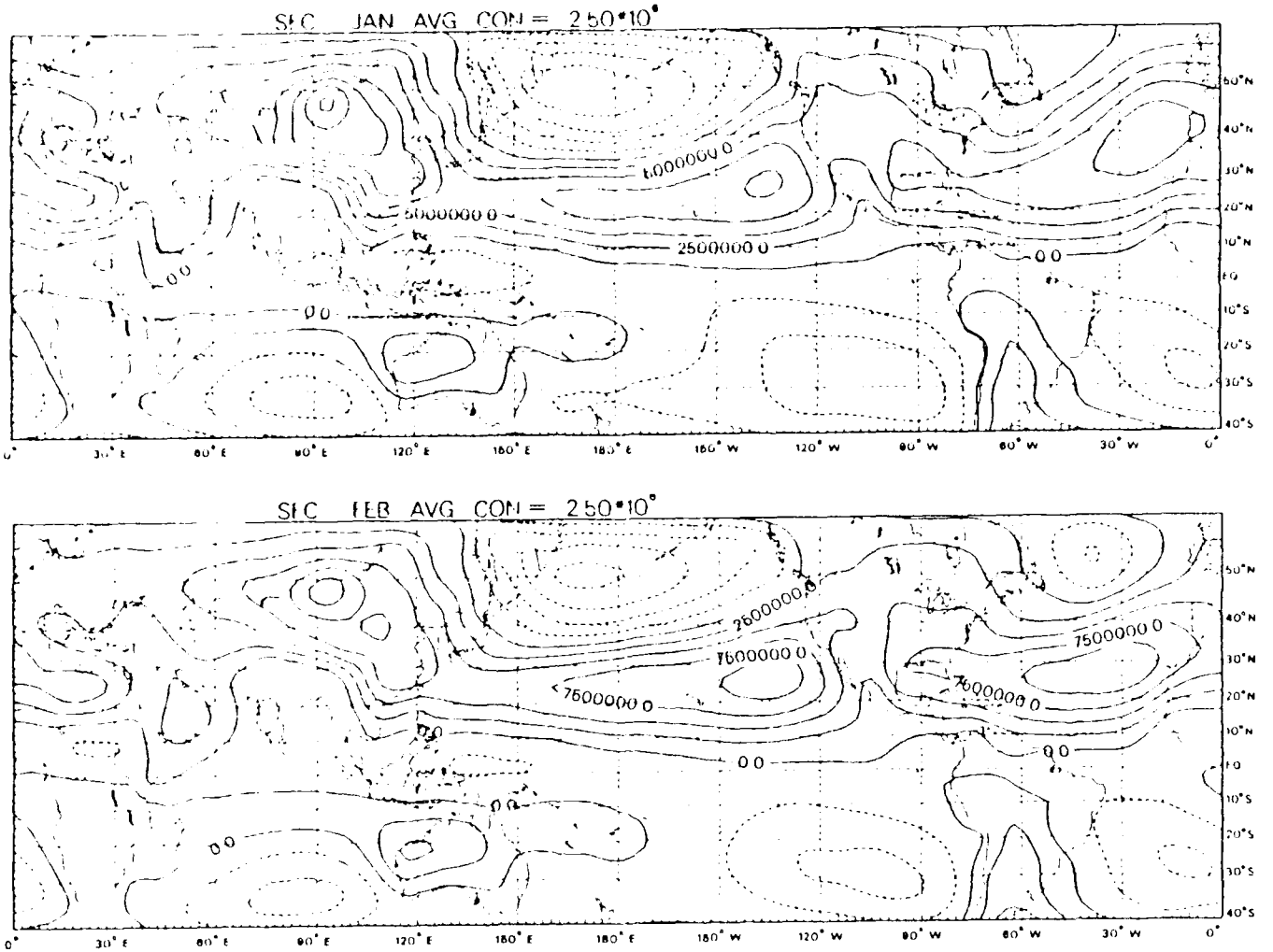
SIC JAN AVG CON = 250*10°
SIC FEB AVG CON = 250*10°
60°N
40°N
30°N
20°N
10°N
EQ
10°S
20°S
30°S
40°S
0°
30° E
60° E
90° E
120° E
180° E
180° W
120° W
90° W
60° W
30° W
0°

Fig. 3.7 (cont'd.)

TABLE III

Summary of cross-spectral analysis of the diurnal cycle.

Base Series = NEM1

(a) Phase

Season	XEF1	XEF2	SSM1
1974-75	0.49	0.48	0.99
1975-76	0.46	-	0.02
1976-77	-	-	0.99
1977-78	0.47	0.48	0.98
1978-79	0.51	0.48	0.01
1979-80	0.46	0.50	0.00
1980-81	-	-	0.99
1981-82	-	-	-
1982-83	-	-	-
AVERAGE	0.48	0.49	0.997

(b) Coherence squared

Season	XEF1	XEF2	SSM1
1974-75	0.10	0.23	0.41
1975-76	0.13	-	0.41
1976-77	-	-	0.48
1977-78	0.37	0.10	0.67
1978-79	0.41	0.21	0.80
1979-80	0.23	0.35	0.74
1980-81	-	-	0.48
1981-82	-	-	-
1982-83	-	-	-
AVERAGE	0.25	0.22	0.57

TABLE II

Summary of date/time of tau=0 for mid- and late-season compositing of area-averaged parameters and surface wind.

Season	Date and Time Mid-season	Date and Time Late-season
1974-75	7 Jan/ 00GMT	6 Feb/ 00GMT
1975-76	31 Dec/ 00GMT	30 Jan/ 00GMT
1976-77	31 Dec/ 12GMT	29 Jan/ 00GMT
1977-78	31 Dec/ 00GMT	13 Jan/ 12GMT
1978-79	21 Dec/ 12GMT	
1979-80	28 Dec/ 00GMT	23 Jan/ 00GMT
1980-81	30 Dec/ 00GMT	
1981-82	8 Jan/ 00GMT	
1982-83	28 Dec/ 00GMT	

Table I (cont'd.)

Parameter	Data and Area	Circulation Components Represented
SSM1	Surface zonal wind over Indonesia-Arafura Sea region (12.5-7.5°S, 115-135°E)	equatorial monsoonal flow
SSM2	Surface zonal wind over Southern New Guinea (12.5-7.5°S, 135-155°E)	equatorial monsoonal flow
SSM3	Surface zonal wind over Honiara and vicinity (12.5-7.5°S, 155-175°E)	equatorial monsoonal flow
WAT	Surface vorticity over Northwestern Australia (27.5-17.5°S, 115-125°E)	surface heat low
SHM	400 mb vorticity over Southwestern Australia (37.5-27.5°S, 115-125°E)	midlatitude mid-tropospheric effect

TABLE I

Area averaged parameters.

Parameter	Data and Area	Circulation Components Represented
NEM1	Surface meridional wind in northern South China Sea (17.5-25°N,105-120°E)	winter monsoon surge
NEM2	Surface meridional wind east of Taiwan/Philippine Islands (17.5-25°N,120-135°E)	winter monsoon surge
NEM3	Surface meridional wind over Guam and vicinity (17.5-25°N,135-150°E)	winter monsoon surge
XEF1	Surface meridional wind over maritime continent (2.5°S-2.5°N,90-120°E)	cross equatorial flow
XEF2	Surface meridional wind north of New Guinea (2.5°S-2.5°N,120-150°E)	cross equatorial flow
XEF3	Surface meridional wind over equatorial Pacific Ocean (2.5°S-2.5°N,150°E-180°)	cross equatorial flow

parameters at fixed periodicities. The exception to this occurred in the diurnal cycle which was known to be prominent in the tropical South China Sea and the maritime continent region (e.g. Johnson, 1982). Table III is a summary of the phases and coherences-squared in the diurnal interval for base series NEM1 crossed with XEF1, XEF2, and SSM1. Only values corresponding to coherence squared greater than 0.1 (coherence greater than 0.32) area listed. Fig. 4.6 shows the average phases and coherences-squared in the diurnal interval for this same base series and crossed circulation features.

The cross spectral analysis demonstrates the following items of interest for the diurnal cycle:

1. NEM1 and SSM1 are coherently in phase.

2. NEM1 and NEM2 have very little coherence indicating that the longitudinal extent of the diurnal cycle is limited to the South China Sea.

3. NEM1 is out of phase with XEF1, XEF2 and WAT, all with moderate coherence.

4. SSM1 and WAt are out of phase with moderate coherence.

A more comprehensive analysis of the three dimensional meteorological variables over the entire region would be necessary to explore the total structure of the diurnal cycle in this region.

The late-season acceleration of the SSM1 parameter is also well correlated with the Southern Hemisphere's midlatitude vorticity at the 400 mb level over southwestern Australia (SHM). There is a significant increase in SHM three days prior to tau=0 and a rapid decrease immediately after tau=0. This may be related to the results suggested by Davidson et.al. (1983) who proposed that major baroclinic develcpment in the Southern Hemisphere midlatitude upper-level takes place prior to the monsoon onset and is a possible forcing mechanism triggering the monsoonal convection north of Australia. Again the events referred to by Davidson et.al. (1983) usually occur in late December versus the mid-January late-season events identified in this study. Nevertheless, both studies suggest a possible role of the Southern Hemisphere midlatitude baroclinic system in influencing tropical monsoonal circulation. It is also probable that these midlatitude activities trigger the surges west of Australia in a manner similar to the northern winter cold surges, which would explain the correspondence found in the surface WAT parameter. Since there is no significant signal in the winter monsoonal flow (NEM1, NEM2, NEM3), as well as, the cross equatorial flow features (XEF1, XEF2, XEF3), this denotes that the late-season event may be a Southern Hemisphere phenomena due to apparent midlatitude baroclinic influences.

Because several time series appear to possess synoptic time scale variations, a cross spectral analysis was performed involving all eleven area-averaged circulation parameters to investigate the possibility that there may be coherent variations at certain frequencies. The time series for analysis covered the period of 00GMT 1 December to 12GMT 25 February (87 days or 174 data points). No consistent results showed up in the various frequency windows which means that there is probably no relationship between the

(>15ms^{-1}) at tau=-72 hours. This is followed by a gradual decrease of the surface northeasterlies, although a region of maximum wind (>10ms^{-1}) persists in the South China Sea throughout the period. The zonal wind along 10°S in the Indonesia-Arafura Sea region is westerly but weak and of little extent before tau=0. After tau=0, the westerlies visibly strengthen and expand eastward from 120°E. The western Australian surface low persists throughout the period. The southerly wind surge along the western Australian coast, although present throughout, shows an enhancement from tau=+72 hours on, with the maximum wind region moving poleward of the surface low. Of note, southeasterly winds present off the northeast coast of Australia, increase in strength at tau=-24 hours. The significance of this increase is unknown and merits further study.

The composited time series of ten circulation parameters for the late-season events are seen in Fig. 4.5. SSM1 again shows a steady acceleration after tau=0 although SSM2 and SSM3 exhibit no significant signal. This limited longitudinal extent of the equatorial monsoonal flow was seen before above although SSM1 is on average stronger during the late-season event. Unlike the mid-season event, the western Australian trough (WAT) is enhanced prior to onset of westerly monsoonal flow. Based on data from the WMONEX year, 1978-79, Davidson (1984) suggested that the Southern Hemisphere's southwesterly surges off the west coast of Australia have a strong influence on the onset of the Australian monsoon convection. The developement of these surges are represented at least partially by the WAT parameter. Even though the onset of the large scale convective blow-up in the Davidson (1984) study is basically a mid-season event, it is possible that a similar mechanism may influence the monsoonal wind changes in the Indonesian region in the late-season events of this study.

and NEM2, the winter monsoon winds within latitudes 17.5-25°N for the regions bounded by 120-135°E and 135-150°E, respectively, show a higher speed prior to tau=0 compared to after tau=0. The signal is much stronger and persists longer in NEM2, with deceleration of the northeasterlies occurring at tau=0. All other circulation parameters (NEM3, XEF1, XEF2, XEF3, SHM, WAT) display no significant signal and, thus, demonstrate no apparent correspondence with the accelerated summer monsoon event.

Examination of the time series of NEM1 and NEM2 for each individual year of data for the same period (tau=-5 days to tau=+6 days) based on the time and data of tau=0 emphasizes the trend seen above. For NEM1, the pre-onset surge of northeasterly winds are clearly delineated in four of the nine-years (1975, 1976, 1980, 1983), weakly delineated in 1977, 1979, 1981 and 1982, and show no signal at all in 1978. For NEM2, the signal is much more apparent which corresponds to the result seen in the composited time series. The signal is clearly seen in seven out of nine-years, with 1977 being weak and 1978 showing no signal at all. This suggests that there is a possible mid-season influence by the northern winter monsoon surge on the equatorial westerlies in the Indonesia- Arafura Sea region. While this influence is detectable over the South China Sea, it most pronounced in the western Pacific Ocean region immediately east of Taiwan and the Philippine Islands.

The phenomena seen in the composited time series are further illustrated in composited maps of surface horizontal wind (Fig. 4.4) for the same period. Maps shown are at 24 hour intervals from tau=-120 hours (tau=-5 days) to tau=+144 hours (tau=+6 days). The choice of 24 hour intervals removes the influence of diurnal effects. The series of composite maps demonstrate a definite increase in the northeasterly monsoonal winds before tau=0 with a maximum

more than five days which occurs after 15 December. This is illustrated using Fig. 4.2 which is the time series of SSM1 for the 1974-75 season where 12GMT 15 December correlates to 30 on the abscissa. This is called the "mid-season" event. There is often another major acceleration event of this zonal wind parameter after the mid-season event which is called the "late-season" event. Since some seasons did not experience a break in southern summer monsoonal flow followed by a recurrent surge of Indonesian monsoonal flow, only five years were chosen as having late-season episodes. Table II gives the specific date and time selected for tau=0 (onset) for each year for both mid- and late-season events.

Based on the timing of the acceleration's initiation, each area-averaged circulation parameter was composited according to a time period of tau=-5 days to tau=+6 days for the mid-season event using the base times for tau=0 defined in Table II. For each parameter, the time series for each year are then composited relative to the tau times. Fig. 4.3 displays the composited time series of ten of the circulation parameters. The surface meridional wind in the vicinity of Guam (17.5-25°N, 135-150°E), NEM3, was not included since it showed no distinguishable signal at all. As expected from our definition of the acceleration event, the base series, SSM1, shows a period of relatively weak westerlies (prior to tau=0), followed by a steep acceleration. This same signal is seen in the surface zonal wind over Southern New Guinea (12.5-7.5°S, 135-155°E), SSM2, although it is somewhat weaker. The signal in the equatorial monsoon flow for the region along 10°S between 155-175°E (SSM3) is very weak, if present at all. This indicates a constraint on the longitudinal extent of the acceleration of the equatorial westerly flow, such that the mid-season event is essentially limited to the vicinity of 115°E to 135°E. Both NEM1

IV. TIME VARIATIONS

The basic analysis involves time series of eleven area-averaged motion parameters constructed to study the time variation of the various circulation components which are deemed to have a possible correlation with the development of the equatorial monsoon winds along 10°S. Table I lists these parameters and the circulation components they represent. The choice of these parameters is based on the monthly mean flow patterns reported in the preceeding chapter. Each parameter shows up as a major circulation feature in the monthly mean charts. Fig. 4.1 shows the areas over which the parameters of Table I were averaged. Area-averages were calculated twice daily for each of these circulation components for the period of 00GMT 1 December to 12GMT 15 February.

The area-averaged zonal wind component of the surface winds over the Indonesia-Arafura Sea region (12.5-7.5°S, 115-135°E), SSM1, is used as the index to determine the relative timing of the major circulation changes with respect to the acceleration of equatorial westerly flow. Examination of the time series of area-averaged SSM1 for each individual year shows that, in addition to diurnal cycles, there are several significant fluctuations in the zonal wind throughout the period which are on the synoptic time scale. Since the onset of the Southern Hemisphere's summer monsoon, regardless of the definition used, usually occurs near the end of December, it was decided to focus on the major acceleration event after 15 December for each year. The initiation of a period of acceleration of equatorial zonal wind along 10°S (tau=0) is chosen to be the relative minima preceding a period of sustained acceleration of

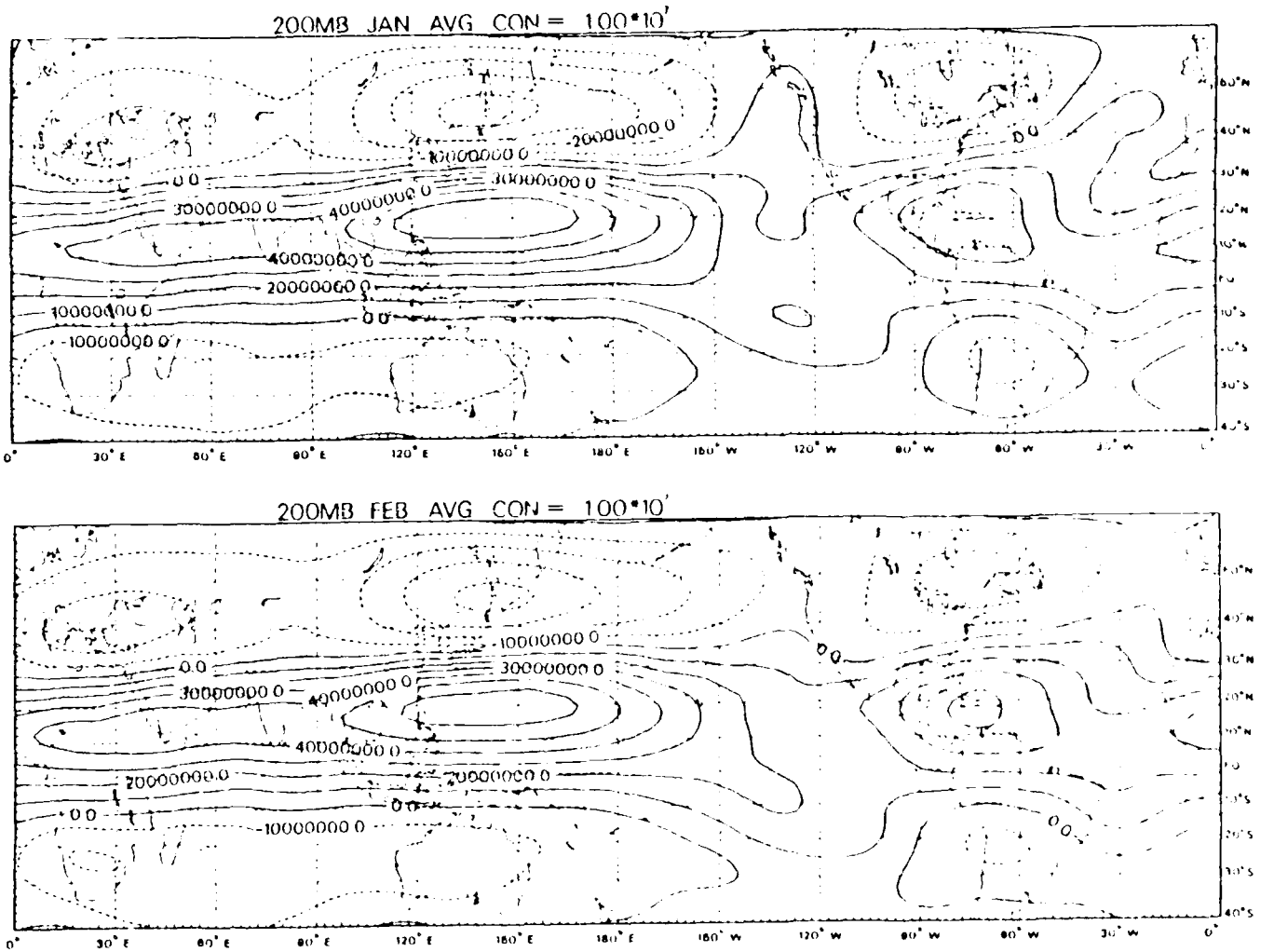

Fig. 3.9 (cont'd.)

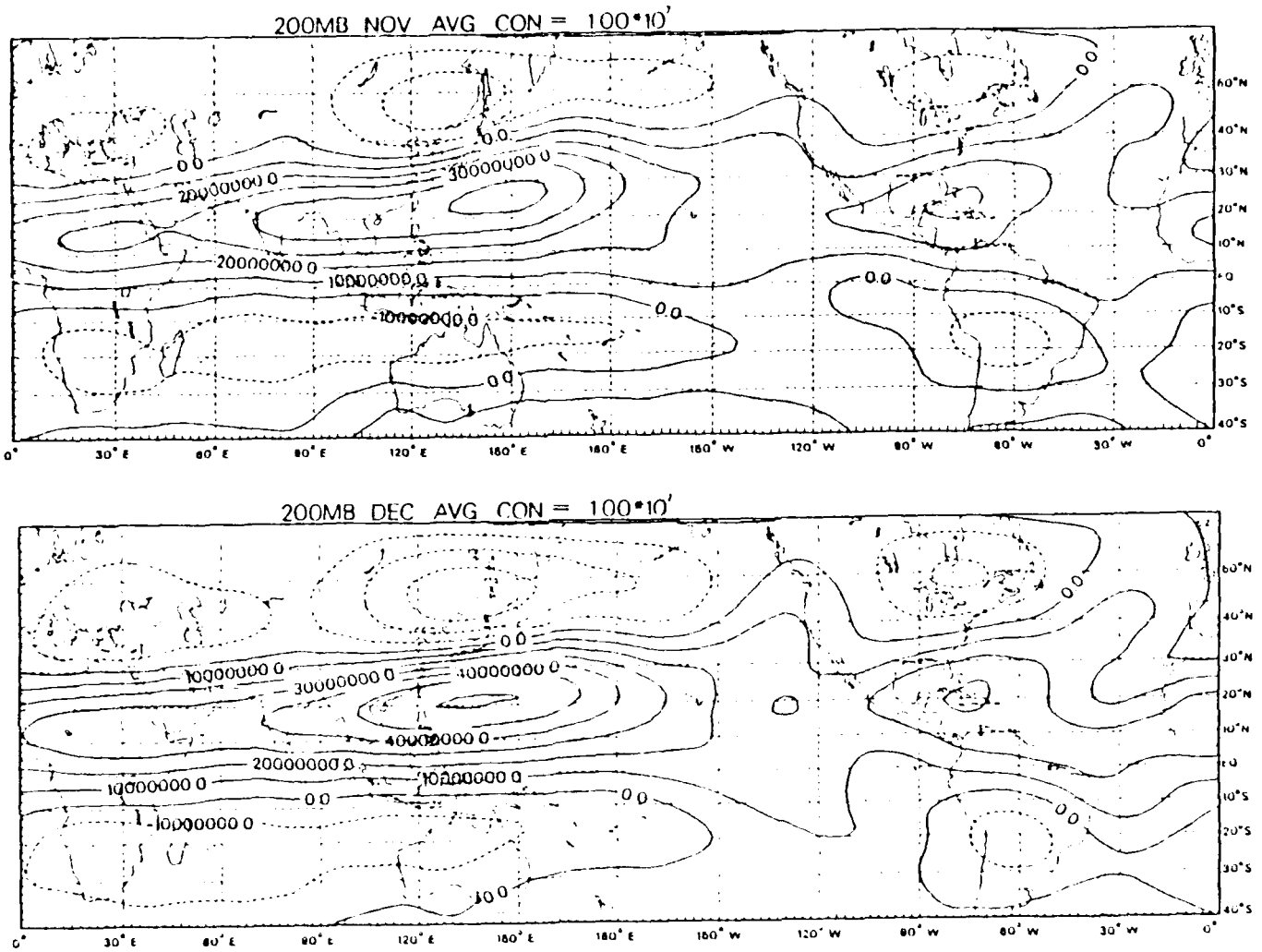

Fig. 3.9 As in Fig. 3.7, except for 200 mb level.

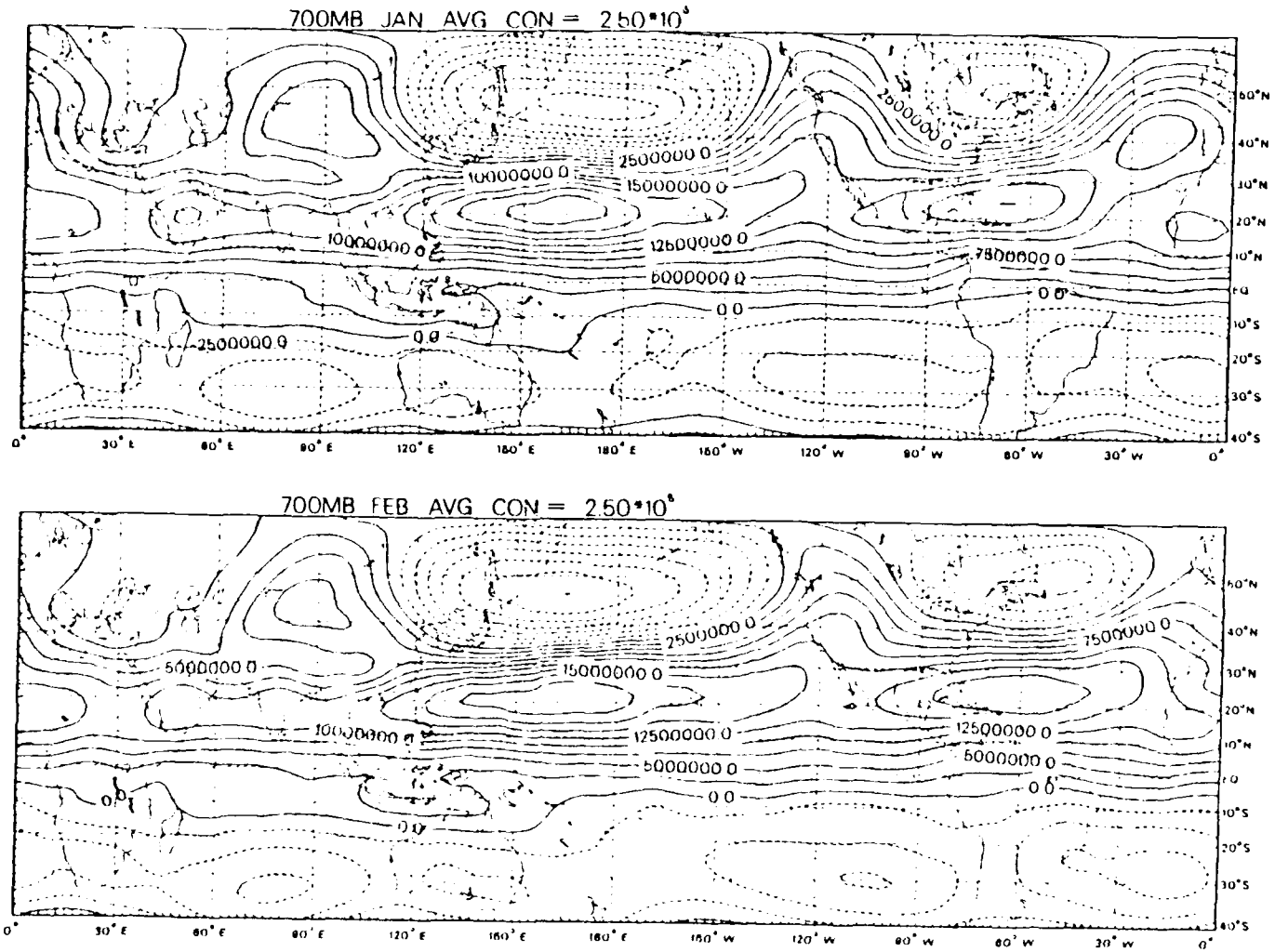
700MB JAN AVG CON = 2.50*10⁵
25000000
10000000
15000000
12500000
7500000
5000000
0.0
700MB FEB AVG CON = 2.50*10⁵
25000000
5000000
15000000
12500000
7500000
10000000
0.0
60°N
40°N
30°N
20°N
10°N
EQ
10°S
20°S
30°S
40°S
0°
30°E
60°E
90°E
120°E
150°E
180°E
150°W
120°W
90°W
60°W
30°W
0°

Fig. 3.8 (cont'd.)

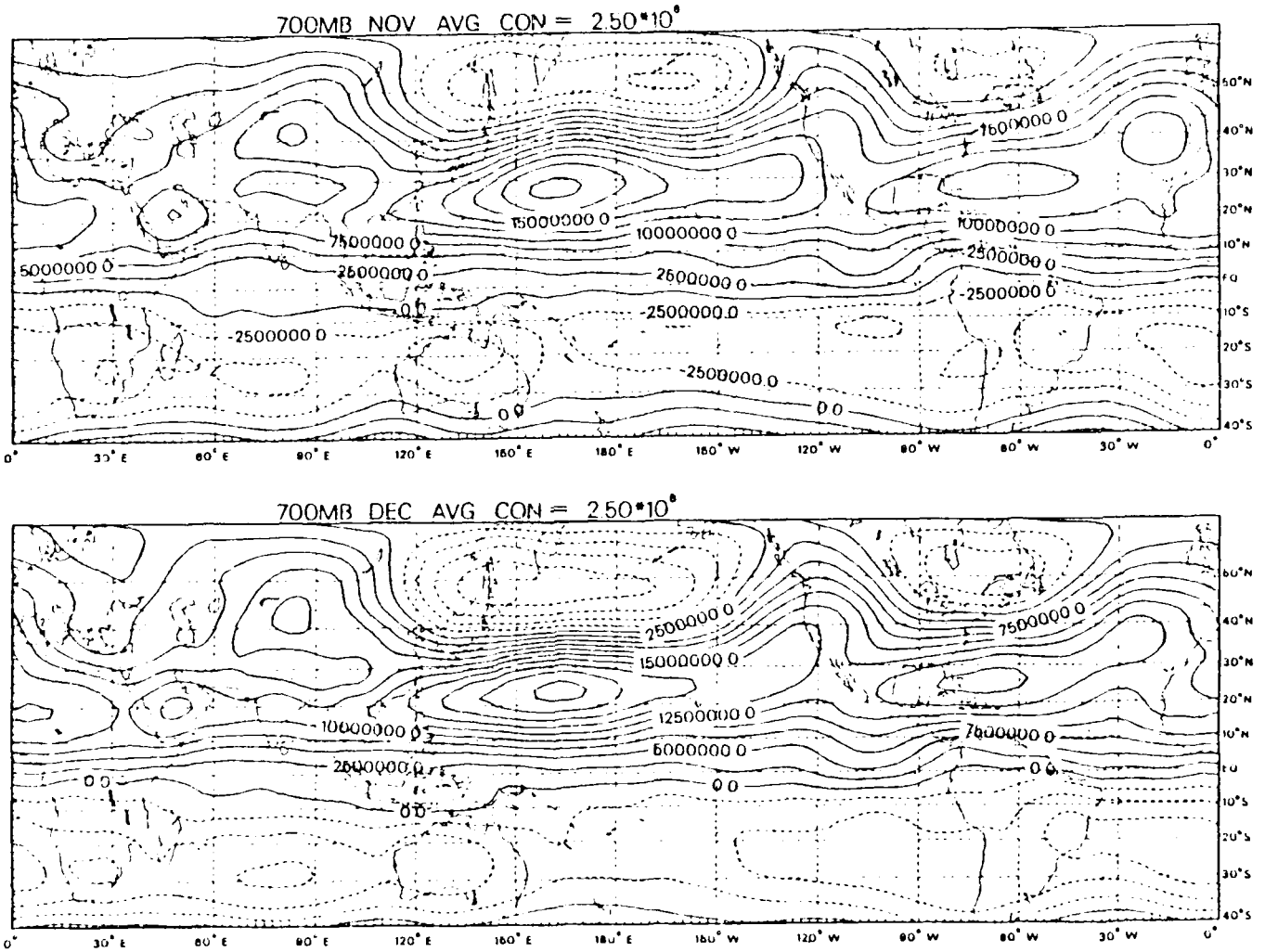

Fig. 3.8 As in Fig. 3.7, except for 700 mb level.

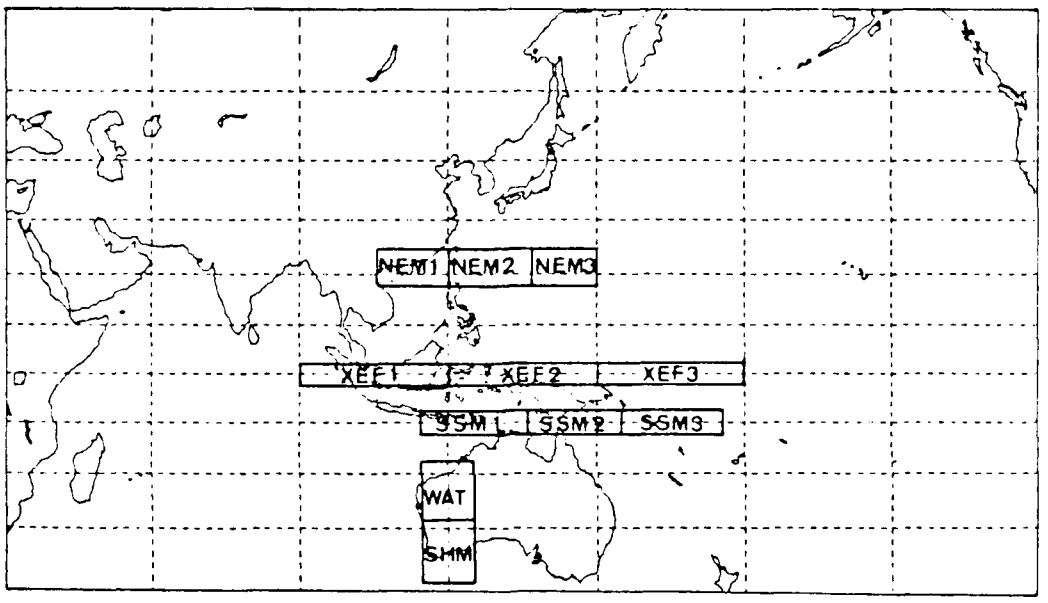

Fig. 4. Map showing different areas over which the parameters indicated are averaged. (See Table I for details)

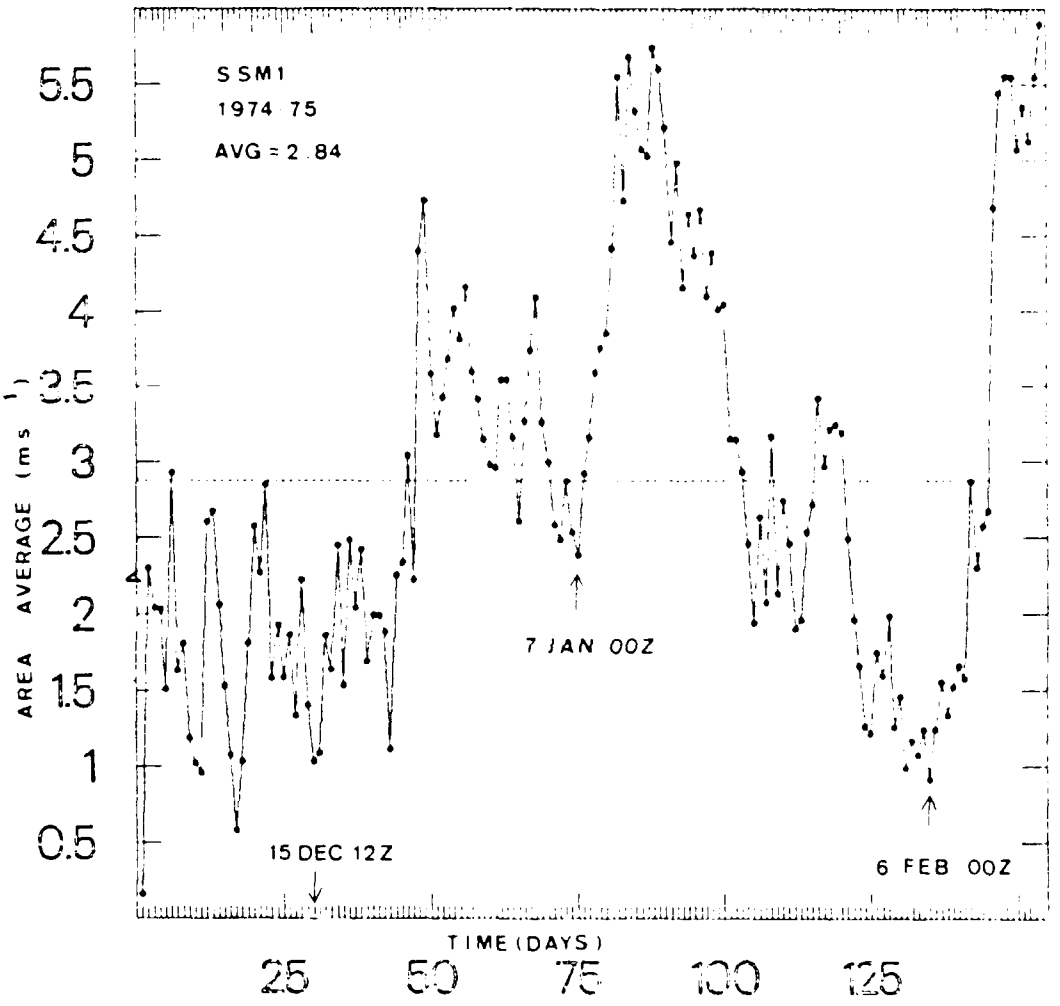

Fig. 4.2 Time series of area-averaged surface zonal wind over the Indonesia-Arafura Sea region (12.5-7.5°S, 115-135°E).

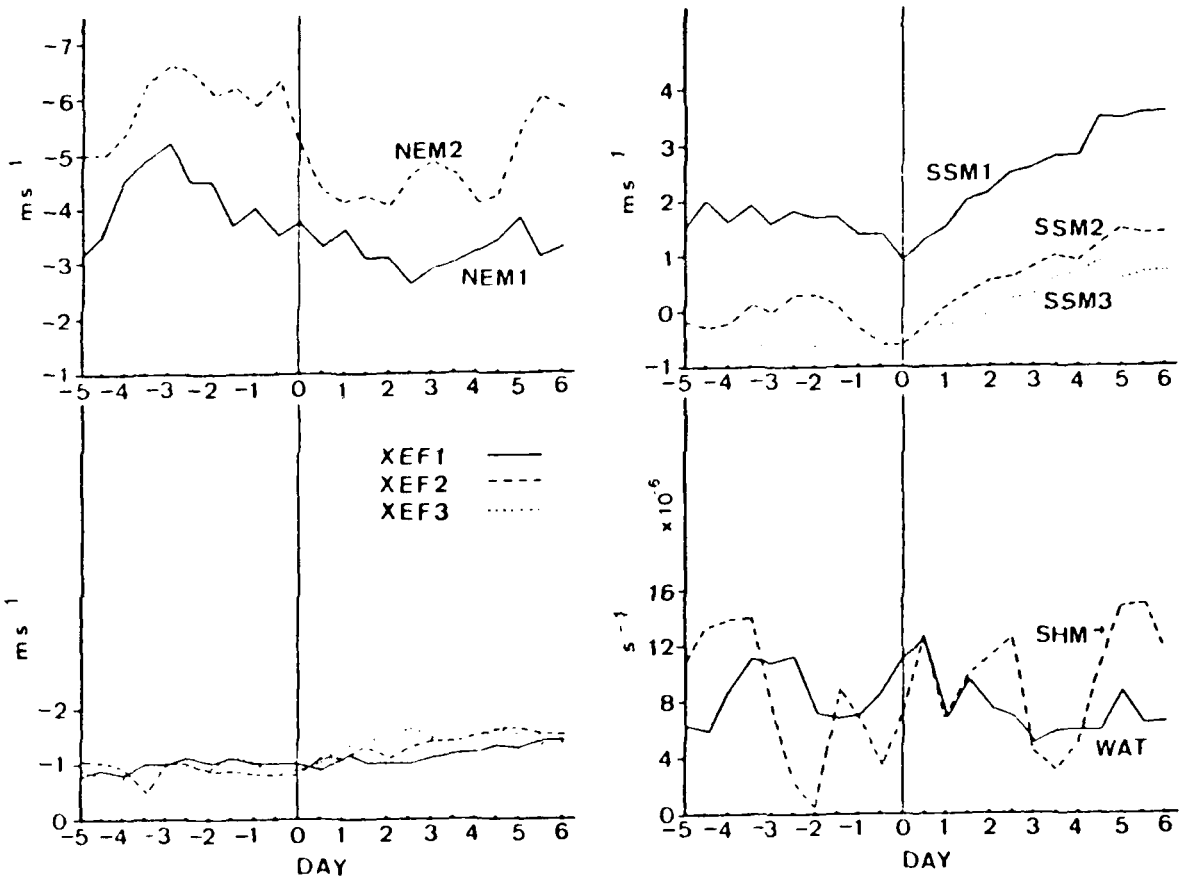

Fig. 4.3 Time series of mid-season composited area averaged parameters. Period from tau=-5 days to tau=+6 days.

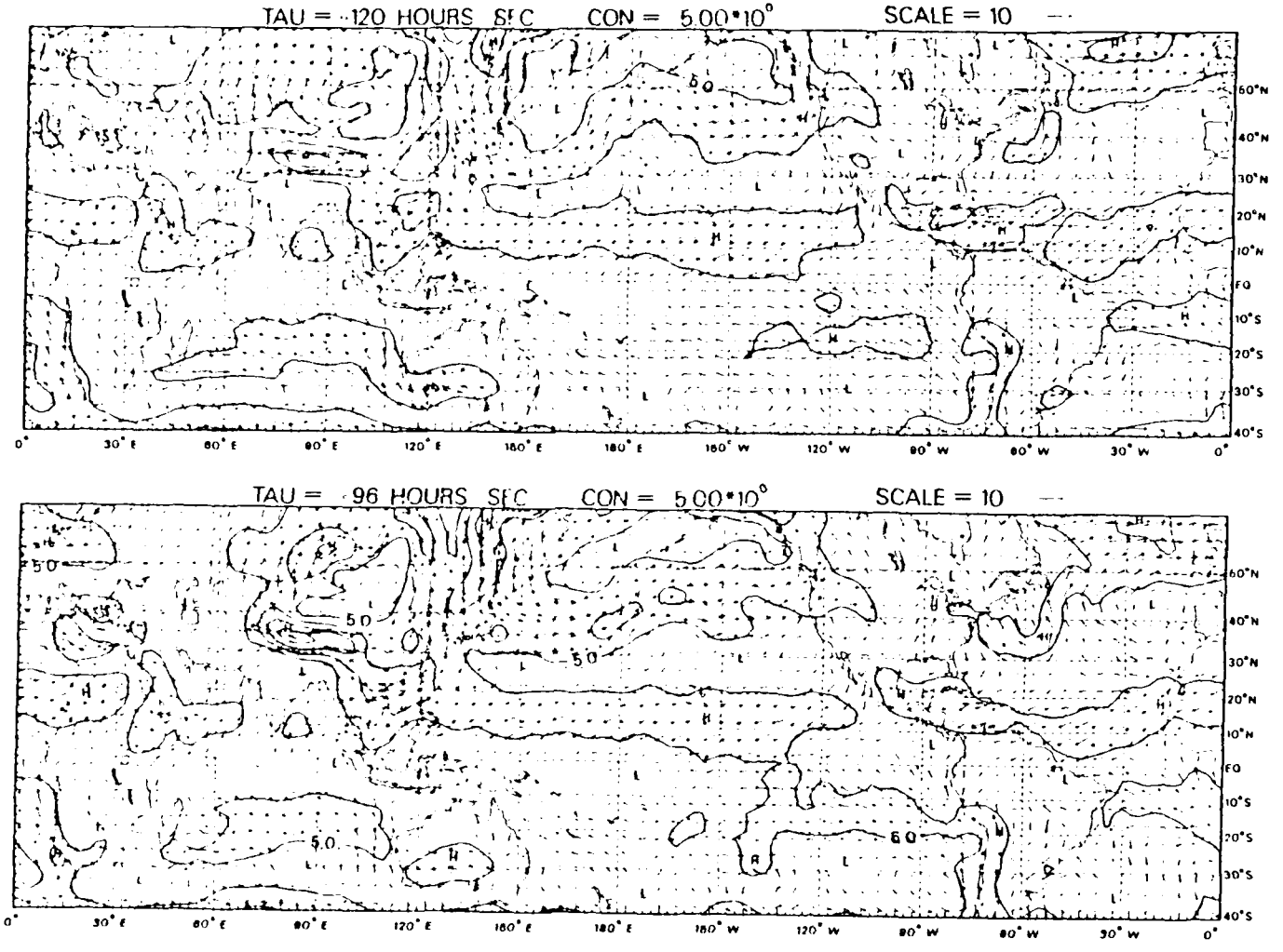

Fig. 4.4 Composite maps of surface horizontal wind at 24-hour time intervals.

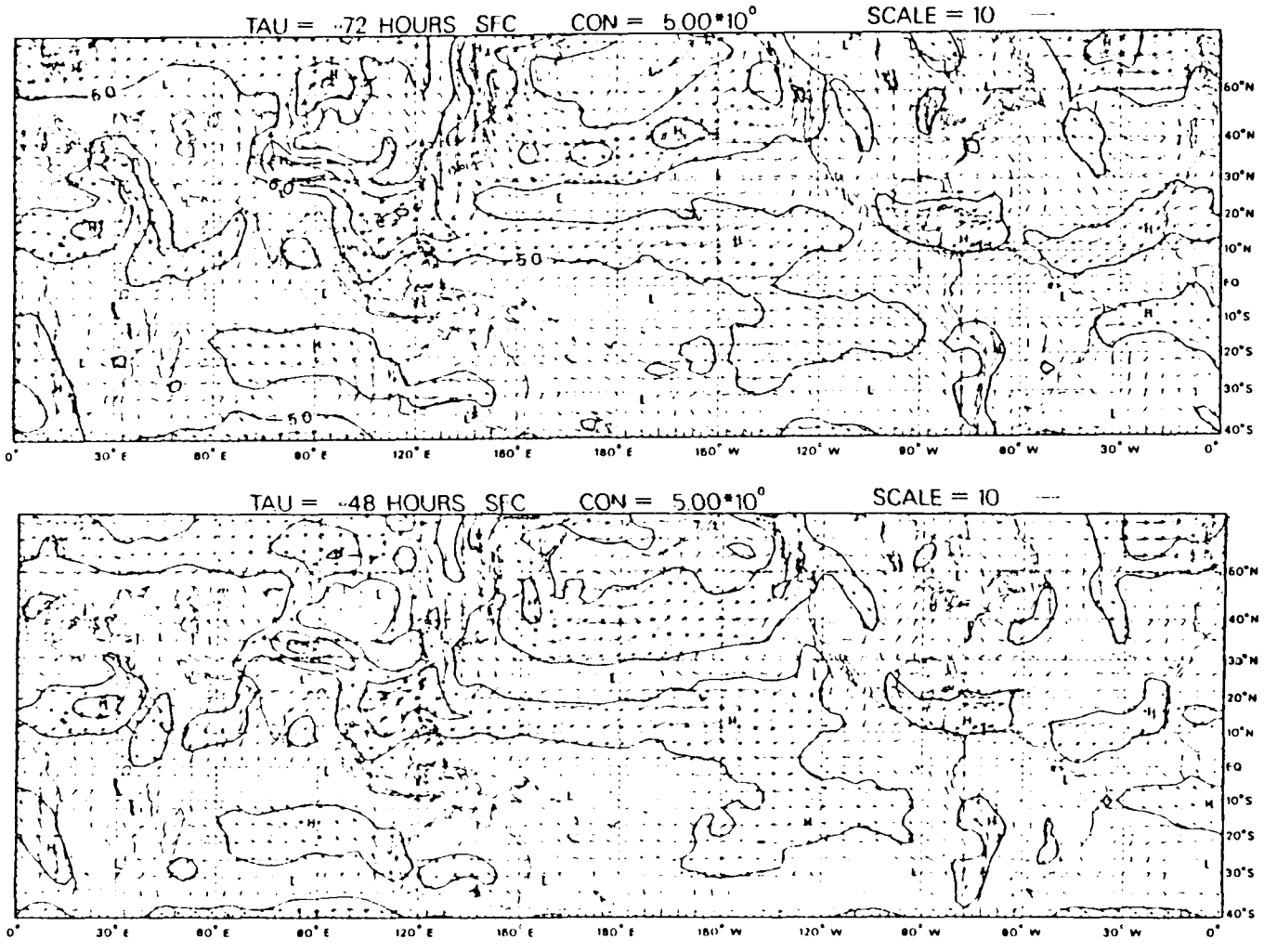
TAU = -72 HOURS SFC CON = 5.00*10^0 SCALE = 10
TAU = -48 HOURS SFC CON = 5.00*10^0 SCALE = 10
60°N
40°N
30°N
20°N
10°N
EQ
10°S
20°S
30°S
40°S
0°
30° E
60° E
90° E
120° E
150° E
180° E
150° W
120° W
90° W
60° W
30° W
0°

Fig. 4.4 (cont'd.)

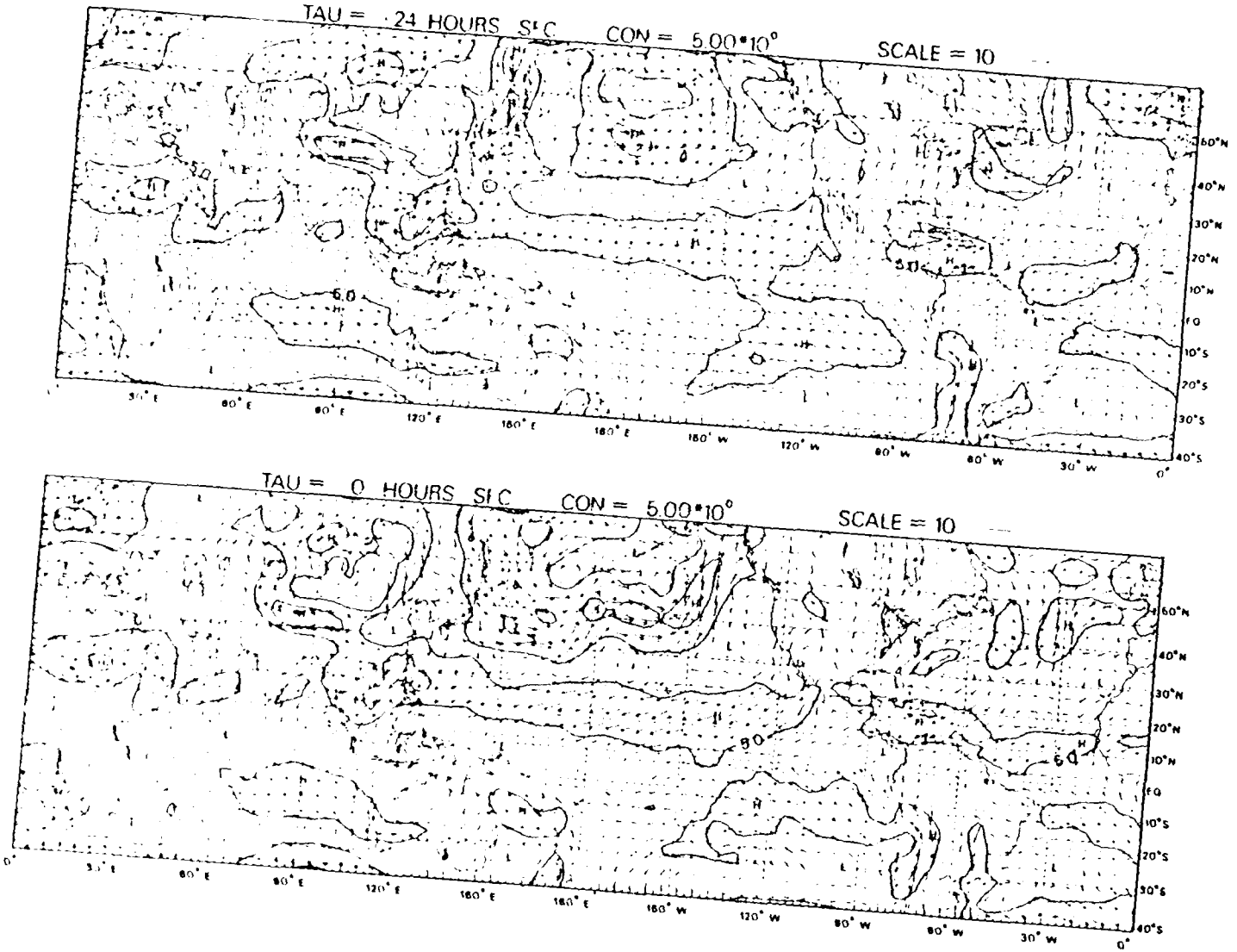
TAU = 24 HOURS SLC CON = 5.00*10°
SCALE = 10
TAU = 0 HOURS SLC CON = 5.00*10°
SCALE = 10

Fig. 4.4 (cont'd.)

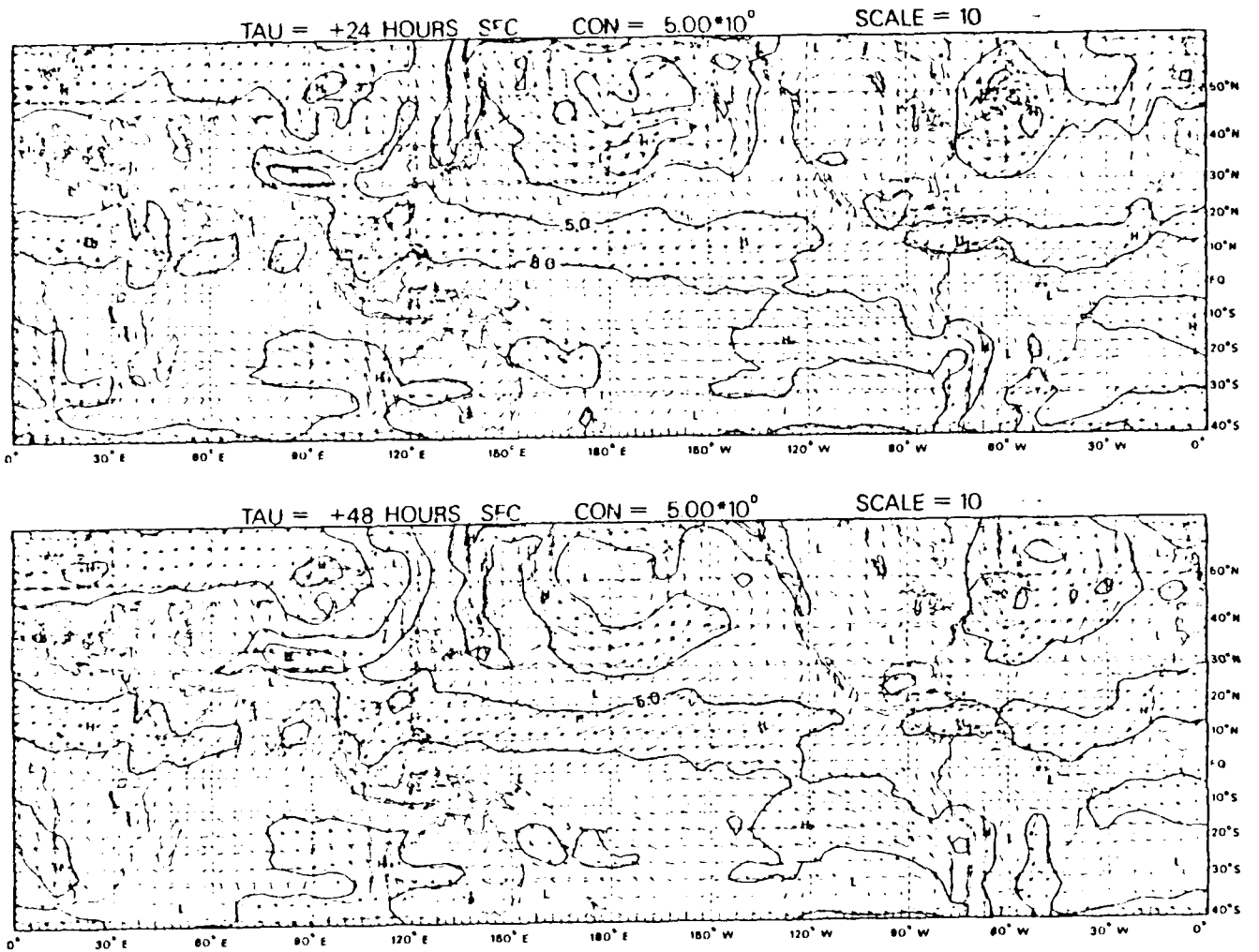
TAU = +24 HOURS SFC CON = 5.00*10° SCALE = 10
5.0
8.0
TAU = +48 HOURS SFC CON = 5.00*10° SCALE = 10
5.0

Fig. 4.4 (cont'd.)

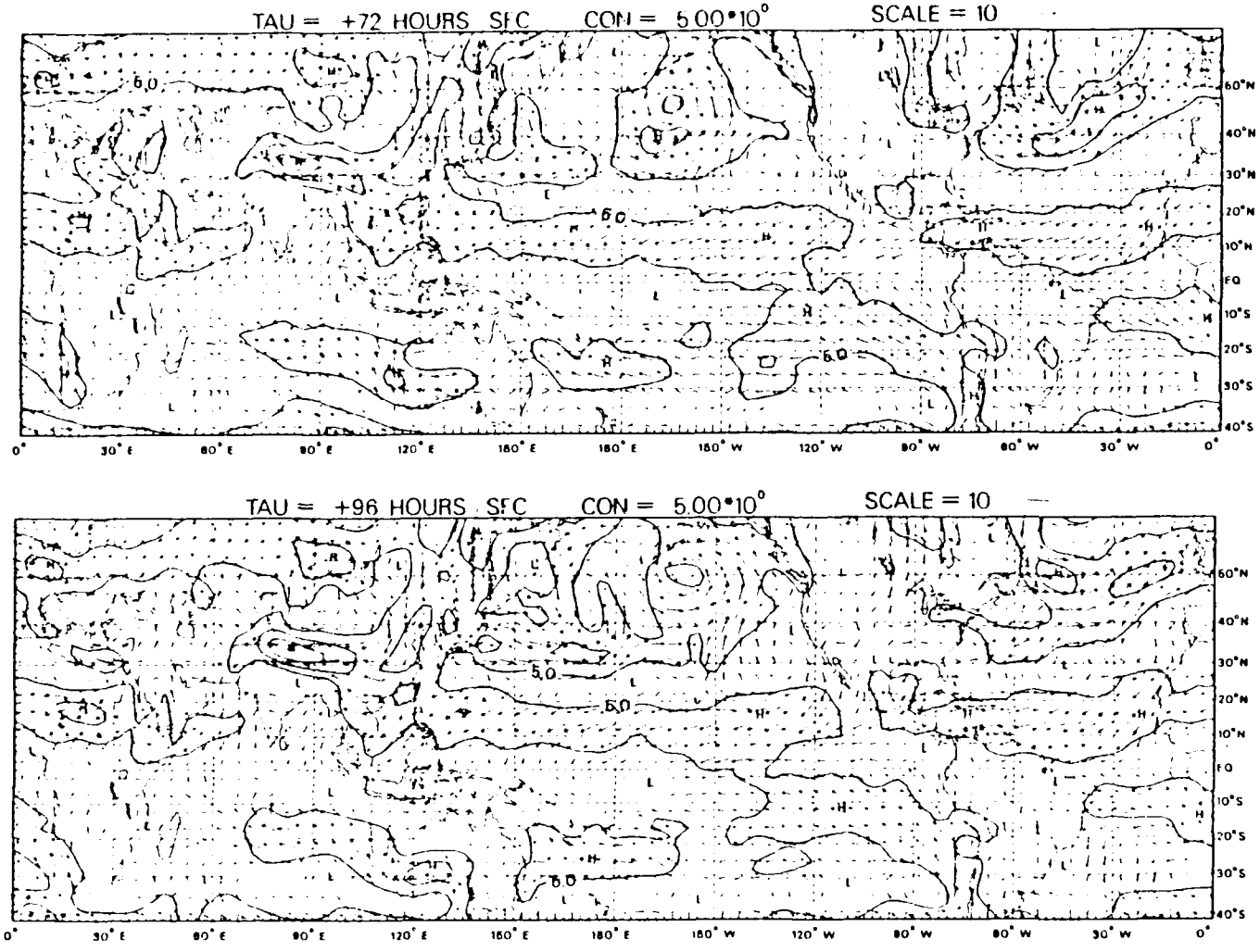
TAU = +72 HOURS SFC CON = 5.00*10^0 SCALE = 10
TAU = +96 HOURS SFC CON = 5.00*10^0 SCALE = 10
5.0
60°N
40°N
30°N
20°N
10°N
EQ
10°S
20°S
30°S
40°S
0°
30° E
60° E
90° E
120° E
150° E
180° E
150° W
120° W
90° W
60° W
30° W
0°

Fig. 4.4 (cont'd.)

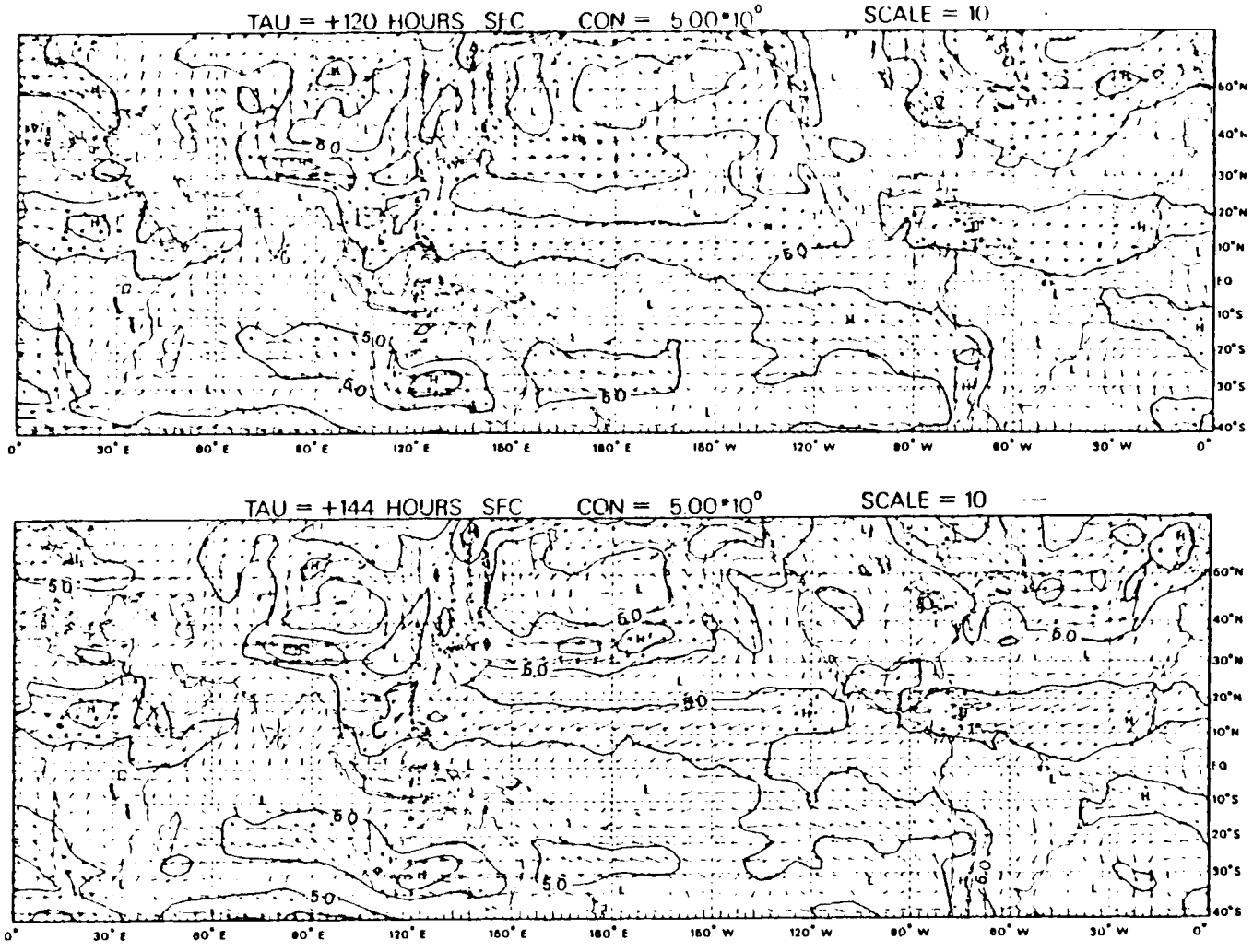
TAU = +120 HOURS SFC CON = 5.00*10°
SCALE = 10
TAU = +144 HOURS SFC CON = 5.00*10°
SCALE = 10

Fig. 4.4 (cont'd.)

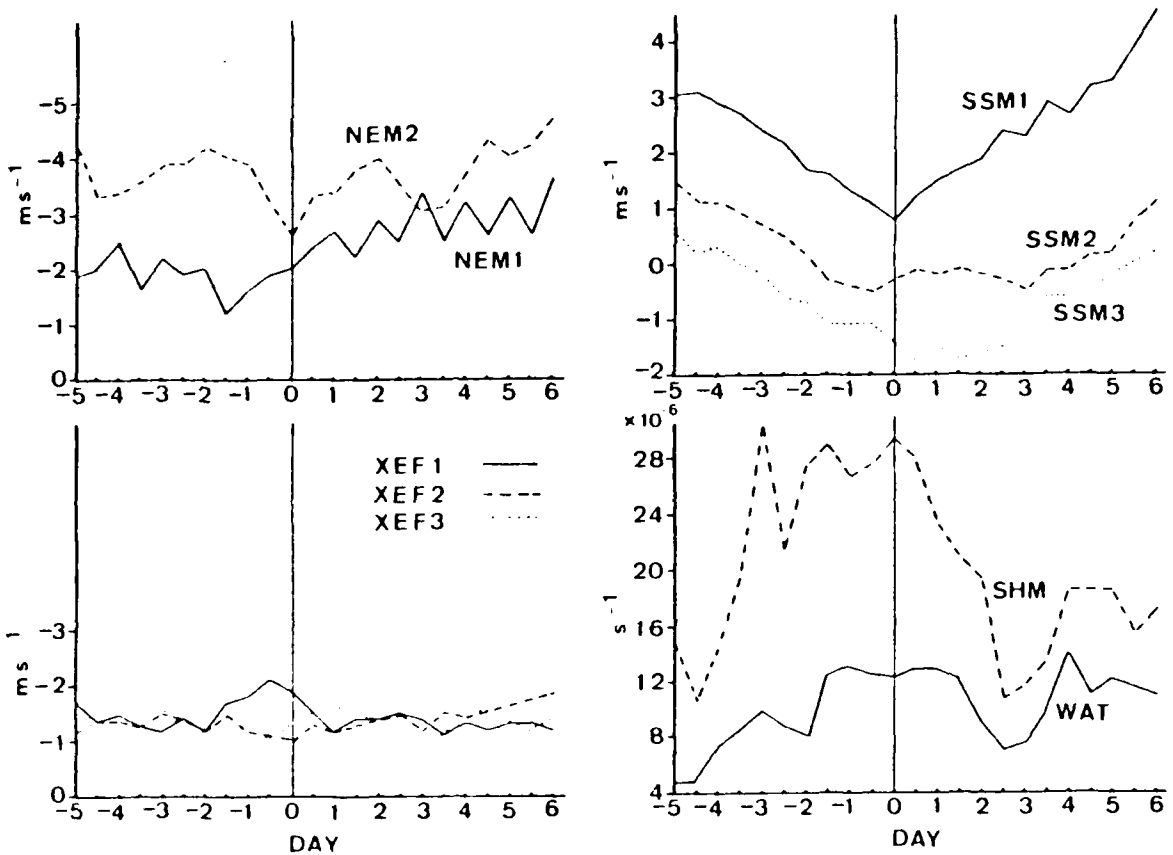

Fig. 4.5 As in Fig. 4.3, except for late-season composited area-averaged parameters.

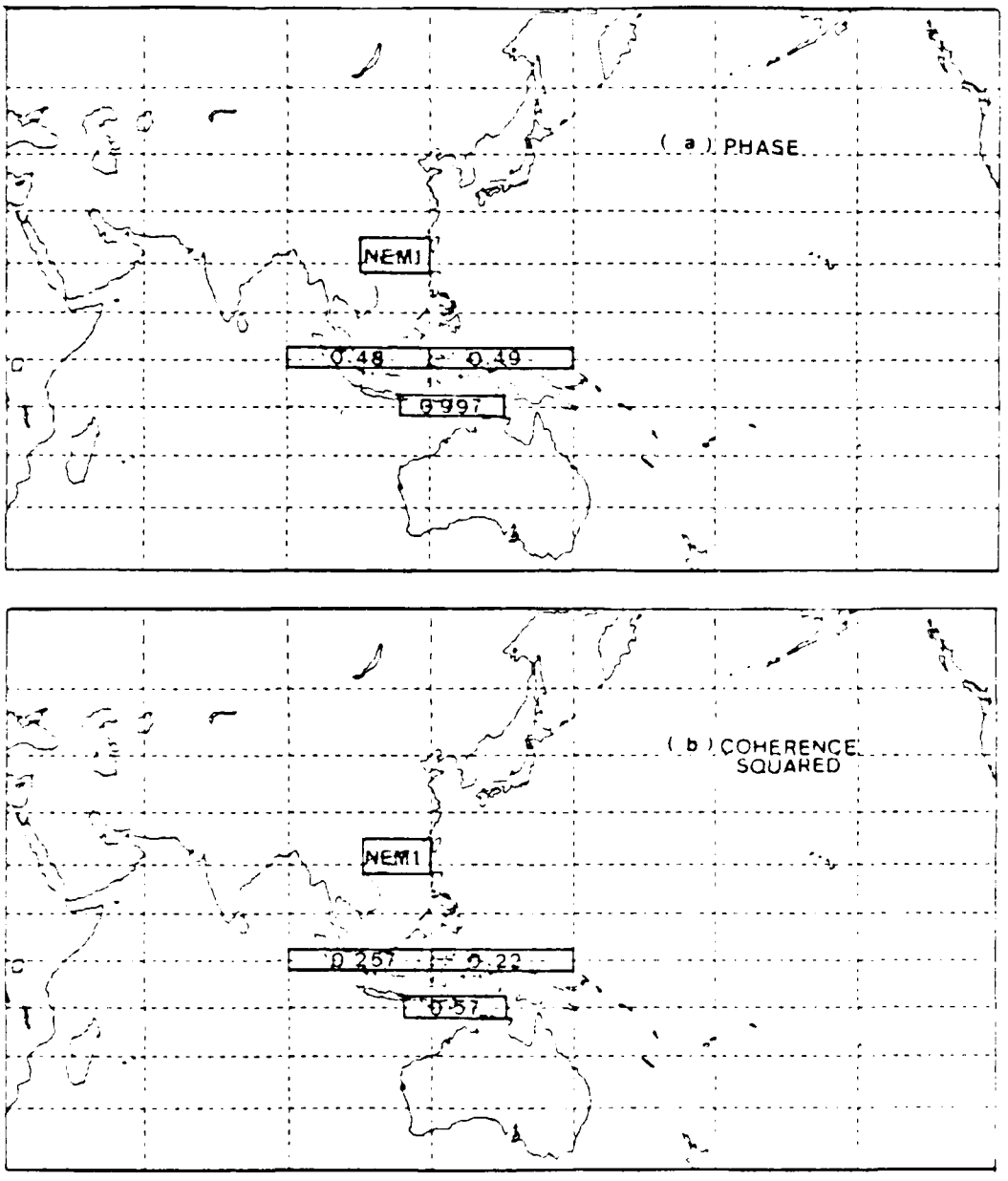

Fig. 4.6 Map of averaged (a) phase and (b) coherence squared of parameters with base time series NEM1.

V. CONCLUSIONS AND RECOMMENDATIONS

The primary objective of this study is to identify the possible cross equatorial influences of the northeast monsoon in the Northern Hemisphere on the Southern Hemisphere's summer monsoon. In addition, the data used in this study were utilized to construct a nine-year monthly mean wind climatology. Using the results of previous work on the Southern Hemisphere's summer monsoon, the acceleration of the southern equatorial zonal winds along 10°S in the Indonesia-Arafura Sea region (SSM1) was chosen as the main parameter to define the timing of the onset (tau=0) of the southern summer monsoon. The initiation of a period of accelerated equatorial zonal wind along 10°S (tau=0) was chosen to be the relative minima preceding a period of sustained acceleration of more than five days occurring after 15 December. Periods of active southern summer monsoon are separated into mid- or late-season events. This distinction in periods of active monsoon is dependent upon whether there was a distinct breaks in the monsoon during the individual season. The criterion for onset defines a period which is a precursor to the enhanced winds and convection, and, hence rainfall which are often used to describe the onset of the Southern Hemisphere summer monsoon over northern Australia.

Time mean circulation charts of wind, velocity potential and streamfunction were compiled. These charts were based on twice daily objectively analysed zonal (u) and meridional (v) wind data of the surface, 700 and 200 mb levels for the months of November through February of a nine-year period covering the winter monsoon seasons of 1974-75 through 1982-83. These charts were used to identify key synoptic

scale, low-level circulation features relevant to this study, the most notable of which is the surface northeast monsoonal winds in the South China Sea, the zonal winds along 10°S in the Indonesia-Arafura Sea region and the western Australian trough. They were also used to define regions for area averaging and compositing of mid- and late-season onset events based on sustained accelerated westerly zonal flow used to define onset (tau=0). Examination of the results of the composited area averaged time series parameters and objectively analysed wind charts and the cross spectral analysis, yield the following conclusions:

1. The surge of surface meridional wind in the South China Sea (NEM1) and the western Pacific Ocean region immediately east of Taiwan and the Philippine Islands (NEM2) are the only area averaged parameters showing a possible signal related to the acceleration of westerly wind along 10°S (SSM1) during the mid-season event. Both NEM1 and NEM2 demonstrate wind surges prior to tau=0 compared to after tau=0. The signal is much stronger and persists longer in NEM2, with a deceleration of northeasterlies occurring at tau=0. All other mid-season circulation features displayed no significant signal.

2. The late-season event appears to be due to a Southern Hemisphere midlatitude, mid-tropospheric phenomena resulting from the baroclinic effect of the upper-level trough in the mid-latitude westerly trades (SHM). The vorticity of the western Australian trough (WAT) enhances at tau=-5 days. There is a possibility that the strengthened trough, resulting in a decrease in surface pressure, causes an increase in cross equatorial northerly flow (XEF1) at tau=-2 days. This sequence is totally a Southern Hemispheric event.

3. In the mid-season event, the zonal wind acceleration is predominantly concentrated in the Indonesia-Arafura Sea region defined by SSM1 and SSM2, while in the late-season event it is concentrated primarily in region SSM1. This implies that westerly monsoonal flow acceleration along 10°S is longitudinally limited.

4. Variability in area averaged signal of NEM3, XEF1, XEF2, and XEF3 is so small that the signal is insignificant in this case. This indicates that cross equatorial flow may not be indicative of the nature of the forcing of the Northern Hemisphere monsoonal winds on the southern summer monsoonal flow along 10°S.

5. Cross-spectral analysis indicates no significant relationship among area averaged parameters except in the diurnal cycle.

The indication of an influence from the strengthening of the northern winter monsoon winds for the mid-season event seems inconsistent with the lack of a signal in the cross equatorial flow parameters. There are several possible explanations for this apparent inconsistency. First, the magnitude of the surface meridional wind is very small (generally 1-2ms^{-1}) with its fluctuations at an even smaller amplitude. These magnitudes are close to the observational errors. Murakami and Sumi's (1982b) study, suggesting the influence of cross equatorial flow, was based on 850 mb winds, which are considerably stronger than the surface winds used in this study. Unfortunately, the Navy's Global Band Analysis does not contain data at this level. Second, it is possible that the analysis scheme smoothed out the wind fluctuations at the equator. Use of station-observed, 850 mb data would clarify these two possibilities. Finally,

a strong signal in cross equatorial flow is not necessarily required to support the idea that the northern winter monsoonal flow influences the southern tropics, because the equator may be a nodal point of a meridional wave mode. Thus, changes in the cross equatorial winds could be neglegible.

During the course of this study other facets of further areas of research were also apparent. Since this study concentrated on the acceleration of zonal flow along 10°S, other onset indicators, such as, rainfall and satellite imagery, should be used to evaluate interhemispheric interactions. Another area was the intra-annual variation of the southern summer monscon using the same basic data set of this study. Incorporated in the study of intra-annual variation, is the possible influence of the El Niño/ Southern Oscillation of which there were two events during this data period (1975-76 and 1982-83). Other areas of interest include the possible role of the southerly surface wind surge along the west Australian coast on the Southern Hemisphere's summer monsoon. The composited maps of the surface winds (Fig. 4.4) of the mid-season event show the possible connection of the southern mid-latitudes with the southern tropics in this region at tau=+24 hours and tau=+48 hours. There was also a surge in the southeasterly winds present of the northeast coast of Australia at tau=-24 hours whose significance, if any, is unknown.

The composited area averaged time series (Fig. 4.3) indicate a correlation between the surge of Northern Hemisphere monsoonal winds in the South China Sea and the monsoonal zonal wind flow along 10°S in the Indonesia-Arafura Sea region. Future investigations should attempt to graphically correlate northern winter and southern summer monsoonal surges of wind with convection and rainfall observed over northern Australia. In addition, the

results presented here indicate that the cross equatorial flow at the surface does not exibit this correlation. Further investigation into this relationship is required. Possible enhancement of the southern summer monsoonal winds is achieved through enhancement of the double Hadley cell within the region.

Other circulation features worthy of further study were observed in the time mean circulation maps (Fig. 3.1 through Fig. 3.9). The convection center over Brazil, although not as strong as that over the maritime continental region, is still a significant synoptic feature. So far, this feature has received little attention other than by South American meteorologists.

LIST OF REFERENCES

Berson, F.A., 1961: Circulation and energy balance in a tropical monsoon. Tellus, 13, 472-485.

Berson, F.A. and A.J. Troup, 1961: On the angular momentum balance in the equatorial trough zone of the eastern hemisphere. Tellus, 13, 66-78.

Boyle, J.S. and K.-M. Lau, 1984: Monthly seasonal climatology over the global tropics and subtropics for the decade 1974 to 1983. Volume II: Outgoinglongwave radiation. NPS Technical Report NPS-63-84-007. Naval Postgraduate School, Monterey, Ca, 58pp.

Chang, C.-P. and K.-M. Lau, 1980: Northeasterly cold surges and near-equatorial disturbances over the winter MONEX area during December 1974. Part II: Planetary-scale aspects. Mon. Wea. Rev., 108, 298-312.

Cressman, G.P., 1959: An operational objective analysis system. Mon. Wea. Rev., 87, 367-374.

Davidson, N.E., J.L. McBride and B.J. McAvaney, 1983: The onset of the Australian Monsoon during winter MONEX: Synoptic aspects. Mon. Wea. Rev., 111, 496-516.

Davidson, N.E., 1984: Short term fluctuations in the Australian Monsoon during winter MONEX. Mon. Wea. Rev., 112, 1697-1708.

Johnson, R.E., 1982: Vertical motion in near-equatorial winter MONEX convection. J. Meteor. Soc. Japan, 60, 682-690.

Holland, G.T., T.D. Keenan and A.E. Guymer, 1984: The Australian monsoon: Definition and variabiltiy. Postprint Volume, 15th Conference on Hurricanes and Tropical Meteorology, Miami, Fl., January 1984. American Meteor. Soc., Boston, Ma., p. 398-402.

Lewis, J.M. and T.H. Grayson, 1972: The adjustment of surface wind and pressure by Sasaki's variational matching technique. J. Appl. Meteor., 11, 586-597.

Lim, H. and C.-P. Chang, 1981: A theory of midlatitude forcing of tropical motions during winter monsoon. J. Atmos. Sci., 38, 2377-2392.

Murakami, T. and A. Sumi, 1982a: Southern hemisphere summer monsoon circulation during the 1978-79 WMONEX. Part I: Monthly mean wind fields. J. Meteor. Soc. Japan, 60, 638-648.

Murakami, T. and A. Sumi, 1982b: Southern hemisphere summer monsoon circulation during the 1978-79 WMONEX. Part II: Onset, active and break monsoons. J. Meteor. Soc. Japan, 60, 649-671.

Oort, A.H., 1983: Global atmospheric circulation statistics, 1958-1973. NOAA Professional Paper 14. U.S. Department of Commerce (available from the Superintendent of Documents, U.S. Government Printing Office, Washington, D.C. 20402).

Ramage, C.S., 1971: Monsoon Meteorology, Academic Press, 296 pp.

Shukla, J. and K.R. Saha, 1974: Computation of non-divergent streamfunction and irrotational velocity potential from observed winds. Mon .Wea .Rev., 102, 419-425.

Troup, A.J., 1961: Variation in upper tropospheric flow associated with the onset of the Australian summer monsoon. Indian J. Meteor. Geophys., 12, 217-230.

INITIAL DISTRIBUTION LIST

		No. Copies
1.	Defense Technical Information Center Cameron Station Alexandria, VA 22314	2
2.	Library, Code 0142 Naval Postgraduate School Monterey, CA 93943	2
3.	Chairman (Code 68Mr) Department of Oceanography Naval Postgraduate School Monterey, CA 93943	1
4.	Chairman (Code 63Rd) Department of Meteorology Naval Postgraduate School Monterey, CA 93943	1
5.	Dr. C.-P. Chang (Code 63Cp) Department of Meteorology Naval Postgraduate School Monterey, CA 93943	2
6.	Dr. J.S. Boyle (Code 63Xj) Department of Meteorology Naval Postgraduate School Monterey, CA 93943	1
7.	Commanding Officer Attn: LT Kathy A. Shield Naval Polar Oceanography Center 4301 Suitland Road Washington, D.C. 20390	1
8.	Director Naval Oceanography Division Naval Observatory 34th and Massachusetts Avenue NW Washington, DC 20390	1
9.	Commander Naval Oceanography Command NSTL Station Bay St. Louis, MS 39522	1
10.	Commanding Officer Naval Oceanographic Office NSTL Station Bay St. Louis, MS 39522	1
11.	Commanding Officer Fleet Numerical Oceanography Center Monterey, CA 93940	1
12.	Commanding Officer Naval Ocean Research and Development Activity NSTL Station Bay St. Louis, MS 39522	1

13. Commanding Officer 1
Naval Environmental Prediction
Research Facility
Monterey, CA 93940

14. Chairman, Oceanography Department 1
U. S. Naval Academy
Annapolis, MD 21402

15. Chief of Naval Research 1
800 N. Quincy Street
Arlington, VA 22217

16. Office of Naval Research (Code 420) 1
Naval Ocean Research and Development
Activity
800 N. Quincy Street
Arlington, VA 22217

17. Commander 1
Oceanographic Systems Pacific
Box 1390
Pearl Harbor, HI 96860

END

FILMED

8-85

DTIC